The performance of pipeline ploughs traversing seabed slopes

Bransby, Mark; Barlow, David T; Brown, Michael; Davidson, John; Brankin, Stuart; Robinson, Scott

Published in:
Ocean Engineering

Publication date:
2018

Document Version
Peer reviewed version

Elsevier Editorial System(tm) for Ocean Engineering

Manuscript Draft

Manuscript Number: OE-D-16-00819R2

Title: The performance of pipeline ploughs traversing seabed slopes

Article Type: Full length article

Keywords: offshore pipeline ploughing; slopes; physical modelling; sand

Corresponding Author: Dr. Michael John Brown, PhD

Corresponding Author's Institution: University of Dundee

First Author: Mark F Bransby, PhD

Order of Authors: Mark F Bransby, PhD; David Barlow, MEng; Michael John Brown, PhD; John Davidson, MSc; Stuart Brankin; Scott Robinson, MEng

Abstract: Ploughing is a method used to bury pipelines beneath the seabed. In this method, a large purpose built plough is pulled by a support vessel to create a trench into which a pipeline is lowered. The soil that has been removed is then placed or back filled over the pipeline to provide thermal insulation, protective cover and to prevent upheaval buckling (UHB) due to pipeline thermal expansion. The majority of previous research effort has focussed on the behaviour of ploughs on level seabeds and has not investigated common geohazards such as sloping seabeds. There is also limited guidance available to industry on the limitations of ploughing on slopes. This paper reports a series of experimental tests conducted to investigate how ploughs may behave when seabed slopes are encountered and ploughing has to traverse cross-slope. The results show that ploughing operations can still be undertaken when traversing a slope but that the efficiency of operations is reduced with increasing slope inclination, leading to a reduction of trench depth and spoil heap sizes on steeper slopes. This may result in reduced pipeline cover depths on slopes if these effects cannot be mitigated.

THE PERFORMANCE OF PIPELINE PLOUGHS TRAVERSING SEABED SLOPES

Manuscript No.: OE-D-16-00819

Revised submission: 19/10/17

M.F. Bransby[a], D.T. Barlow[a,] M.J Brown[a], J. Davidson[a], S. Brankin[a] and S. Robinson[a]

[a] Civil Engineering, University of Dundee, DD1 4HN, UK

Abstract

Ploughing is a method used to bury pipelines beneath the seabed. In this method, a large purpose built plough is pulled by a support vessel to create a trench into which a pipeline is lowered. The soil that has been removed is then placed or back filled over the pipeline to provide thermal insulation, protective cover and to prevent upheaval buckling (UHB) due to pipeline thermal expansion. The majority of previous research effort has focussed on the behaviour of ploughs on level seabeds and has not investigated common geohazards such as sloping seabeds. There is also limited guidance available to industry on the limitations of ploughing on slopes. This paper reports a series of experimental tests conducted to investigate how ploughs may behave when seabed slopes are encountered and ploughing has to traverse cross-slope. The results show that ploughing operations can still be undertaken when traversing a slope but that the efficiency of operations is reduced with increasing slope inclination, leading to a reduction of trench depth and spoil heap sizes on steeper slopes. This may result in reduced pipeline cover depths on slopes if these effects cannot be mitigated.

Keywords: offshore pipeline ploughing, slopes, physical modelling, sand

1. INTRODUCTION

Offshore pipelines are often buried within the seabed in order to protect them from fishing activity, boat anchors, environmental loading and to mitigate upheaval buckling (UHB). One method of post-lay burial is to create a trench into which the pipeline is lowered by pulling a large "V" shaped plough through the seabed (Palmer et al., 1979) using a trenching support vessel. Burial of the pipeline can be achieved by running a backfill plough over the pipeline route and pushing the spoil heaps, generated at the edge of the trench, back into the trench (Cathie et al., 1998). The method has the advantage of being able to bury a plough in a wide range of soil conditions, in a continuous process with little mechanical intervention. Typical ploughing rates may be in the range of 150-1000 m/hour, but will be slowed if more difficult soil conditions are encountered such as dense, silty sand (Cathie and Wintgens, 2001) where mobilisation of the maximum support vessel tow force (bollard pull) will limit the rate of progress. To avoid slow progress (or reduce tow force) it is normal in these soil conditions to limit the ploughed depth to 1.5 m below seabed. Where deeper ploughing is required a multi-pass approach is often used to avoid these issues (Machin, 1995) or the use of new generation high bollard pull vessels.

Following installation, the pipeline is likely to be used to transport high-temperature hydrocarbons. This causes a temperature change which may lead to upheaval if insufficient vertical soil restraint is supplied by the soil cover (Morrow and Larkin, 2007). Upheaval buckling is exacerbated with initial imperfections of the pipeline due to 'out-of-straightness (OOS)' (i.e. a lack of level trench leading to reduced soil cover) of the trench base (Cathie et al., 2005). Consequently, the required depth of cover is dependent on the properties of the soil backfill and the out-of-straightness achieved during trenching. The out-of-straightness may be significantly influenced be the plough encountering various seabed geohazards such as sand waves or sloping seabeds for instance.

The current understanding of offshore pipeline plough behaviour has been gathered from small-scale beach tests (Grinsted, 1985, Reece and Grinsted, 1986), back-analysis of ploughing projects (Cathie and Wintgens, 2001) or by laboratory testing at various scales (Bransby et al., 2005, Brown et al., 2006, Lauder et al., 2013). Initial attempts have been made to investigate behaviour using numerical simulations (Peng and Bransby, 2011) but these efforts are limited by the large strain nature of the problem (Cortis et al., 2017) or have focused on structural performance of the plough (Wang et al., 2015). Beach tests and back analysis of trenching projects have the uncertainty of unknown soil properties (e.g. typical geotechnical site investigation may only involve one cone penetration test (CPT) per kilometre for a pipeline route) and the difficulty of deconvoluting the elements of plough

behaviour. Alternatively, 1g scaled laboratory simulations and testing has the advantage of allowing careful control of both soil conditions (e.g. soil types, relative density, surface profile) and plough settings (e.g. plough depth and velocity) to allow parametric study, albeit introducing the need to consider scaling issues (Lauder and Brown, 2014). By combining these and other findings there is relatively good understanding of the force-trench depth-velocity relationships in uniform, level seabed conditions (Palmer, 1999, Cathie & Wintgens, 2001, Lauder et al., 2012, Lauder et al., 2013).

To date though very little work has been carried out examining the effect of geohazards for example either non-uniform seabeds (i.e. layered soils) (Bransby et al., 2005) or non-level seabed surfaces on pipeline plough performance. The study of non-level or inclined seabeds has previously focused on the investigation of the performance of ploughs in sand wave fields (Allan, 2000, Chen et al., 2001, Bransby et al., 2010) but has not considered seabed slopes. There is little current guidance in the public domain on the offshore industry's approach to ploughing on slopes (down or across) or how decisions are made on the viability of ploughing on slopes. Anecdotal evidence suggests that normally cross slope ploughing on slopes up to 5º does not pose any significant risk to operations but that at slopes steeper than this specific assessment of viability is required. With this apparent lack of guidance to allow industry to make informed decision making on cross slope ploughing (which might be encountered on continental slopes or in smaller geohazards, e.g. pock marks, iceberg scour etc.). the response of ploughs traversing slopes has been investigated by performing a series of 1/50th-scale laboratory tests in which the slope angle was varied from 0 to 30°. This paper reports the experimental methods used, the results obtained and discussion of implications for ploughing practice.

2. EXPERIMENTAL PLOUGH MODELLING

2. 1 Introduction

Before presenting the experimental methodology, the conditions investigated in the experiments are first introduced. A pipeline can cross a slope in three ways: (i) by traversing it, (ii) by going directly up or down the slope line, or (iii) by going obliquely up or down and across the slope. Clearly, the third case is the general one, where an angle of incidence to the slope fall line could be used to define all cases. Case (ii) is likely to be the worst in terms of changes in tow force as tow forces are likely to increase with slope angle if going uphill. Case (i), traversing the slope is likely to give the biggest problems in terms of plough roll, spoil heap stability and availability for back filling and this is studied in this paper. The typical geometry and definition of terms for the problem is shown in Fig. 1. The main performance indicators investigated were the influence of slope inclination on tow force, plough depth and position, trench depth and position and the availability of spoil for backfilling. Seven different slope conditions were studied corresponding to slope angles, β = 0, 5, 10, 15, 20, 25 and 30° (Table 1 & 2). It is acknowledged that a 30° slope angle may be considered too steep for

ploughing in practice but this high slope angle was adopted to explore the extremes of behaviour and to investigate plough performance when the slope angle is close to the critical state friction angle of the soil.

Apart from varying the slope inclination the effect of initial plough depth was also considered. This can be fixed on the model ploughs at the beginning of testing (Fig. 2) by changing the inclination of the mounting arm for the front skids. In this study this was set at the beginning of each test to allow two different initial plough settings to be considered resulting in average plough depths of 20.36 mm and 28.07 mm defined for the flat sea bed case. Where plough depth is defined as as the vertical distance between the deepest part of the plough and the initial soil surface level. For the $1/50^{th}$ scale (N=50) model plough used in this study this corresponds to prototype depths of 1.018 m and 1.404 m (where N times the model length gives the prototype length, scaling discussed later) which are consistent with shallow and medium ploughing depths for typical ploughing infrastructure. For depths greater than 1.5 m and depending on the soil conditions multi-pass ploughing is often used (Machin, 1995) or the mobilisation of high bollard pull vessels (with consequent required modifications to a plough to allow deeper ploughing) so deeper ploughing was not considered appropriate for this study. The seabed slopes were formed in loose dry sand to avoid velocity or rate effects during ploughing.

The plough model was based on the geometry and mass of a plough of 208 tonnes and of overall length 16.85 m. At 1/50th scale (i.e. scaling factor N = 50) used in the 1-g laboratory tests, this corresponded to a length of 337 mm and weight, W = 16.3 N (Fig. 1). Previous studies of model ploughing (e.g. Lauder et al., 2013) with particular focus on scaling (Lauder and Brown, 2014) have developed scaling factors which can be used to convert the results of model testing to prototype values. All results shown in this paper are shown at model scale. In this case, the key dimensions that are scaled are lengths or distances which are scaled up by multiplying by N and forces which are increased by N^3. As the tow forces measured during a test are either proportional to the projected area of the plough multiplied by a shear stress or due to soil self-weight, in either case, the model forces will need to be multiplied by 50^3 to recreate full scale behaviour. This is because the area will be reduced by 50^2 and the shear stress by a factor of 50, thus the model tow forces will be $1/50^3$ ($=(1/50^2) \times (1/50)$) times the field tow forces (Brown et al., 2006). The validity of this assumption has previously been verified by Lauder et al., (2013) by comparison of model plough performance over a range of scales to full scale behaviour (Lauder and Brown, 2014).

2.2 Model plough test set up

The 1g model test apparatus was described by Lauder et al., (2013) and is shown in Fig. 3a. Tests were undertaken using a scaled model plough at $1/50^{th}$ scale. A soil container of length 2 m, breadth 0.5 m and depth 0.5 m contained a uniform soil sample. The plough was towed using a flexible tow wire attached to a translating tow point. The towing point was rigidly connected to a trolley which

translated along the top of the container parallel to the soil surface. The trolley was actuated with a pulley system (see Fig. 3a) with a winch powered by a DC motor. In this system, the tow angle was constant once steady-state ploughing conditions were achieved and gave repeatable results in terms of trench depth and tow force in different conditions (Lauder et al., 2013). The length of the soil container was designed to allow steady state conditions i.e. constant plough depth and tow force with corresponding fully formed spoil heaps. Box end effects are avoided with the arrangement as the trolley and tow line maintain a minimum separation between the end of the box and the plough tip of 650 mm or 5.7 plough share lengths.

2.3 Soil bed preparation and material properties

The seabed soil was modelled with a uniform, fine silica sand (Congleton HST95, supplied by WBB Minerals, UK) with D_{50} = 0.14 mm, D_{10} = 0.10 mm, ρ_{max} = 1792 kg/m^3 and ρ_{min} = 1487 kg/m^3. Direct shear testing revealed that ϕ'_{crit} = 32° and the interface friction angle between the plough steel and the sand was 24° (Lauder et al., 2013). All samples were initially prepared loose by stirring to give a uniform samples ($D_r \approx 26\%$; ρ = 1557 kg/m^3). After creating the approximate slope conditions, the exact slope angle was achieved by using a screed plate with a base with the appropriate angle β to the horizontal which was dragged across the soil surface along the length of the box. Following this procedure, the soil sample height was measured at multiple places to ensure that the soil surface level and slope were appropriate and to give reference heights for comparison with later trench measurements.

2.4 Instrumentation

During each test the tow force and the plough position and orientation were measured as the plough was pulled through the model seabed. Tow force was measured with an S-shaped load cell with a capacity of 50 N which was rigidly connected to the base of the tow point on the trolley. The free end of the load cell was connected to the tow line which was connected to the plough.

During ploughing, the plough has six degrees of freedom of movement. Three degrees of freedom are in translation: in the direction of ploughing, Δx; vertically, Δz; and perpendicular to the direction of ploughing (up or down-slope), Δy. The plough is also free to rotate in pitch, roll and yaw. In the tests, four of these types of movement were measured directly.

Movement in the ploughing direction (Δx) was measured using a draw wire transducer ('DWT' in Fig. 3a) with a range of 2000 mm. Vertical movement (Δz) was measured using a linearly variable differential transformer (LVDT), which was positioned with its axis vertical, attached to the translating trolley. Its spindle was placed on a flat plate above the share near the back of the plough

(Fig. 3a, b) to measure the movement of this part of the plough. Translation out of the plane of Fig. 3a (Δy) was not measured directly.

Rotation about the two horizontal axes, pitch and roll, were measured using electronic clinometers (see Fig. 3b). These had an accuracy of 0.1° and were calibrated before testing. They were each mounted to a plate which was connected rigidly to the beam of the plough so they would follow the movements of the plough body. Change of level between the front and back of the plough, pitch θ, has been seen to be important in terms of how a plough cuts a trench (Lauder et al., 2012, Lauder et al., 2013) and is the key component of depth selection by the plough using the long-beam principle (Palmer et al., 1979). Positive pitch was defined as when the base of the share was inclined so that the front cutting portion ('share tip') was lower than the back portion ('share heel'). A zero pitch $\theta = 0$ (as shown in Fig. 2a) occurred when both the share tip and heel were at the same level. Roll, α was measured with a second clinometer (Fig. 3b). A positive roll occurred when the plough followed the inclination of the slope (i.e. a clockwise rotation about the long axis of the plough in Fig. 3b) and $\alpha = 0$ occurs when the elevation of each skid centre is the same. Yaw, δ (rotation about a vertical axis) was not measured directly and will be discussed later in the paper.

2.5. Testing methodology

Once the sample was prepared, the plough was positioned. It was placed on the far left (Fig. 3a) of the container and on the centre-line of the box whilst being orientated so that the plough would move directly across the line of the slope (i.e. in the line of the longest section of the box). No pre-embedment (Brown et al., 2006) was attempted. The skids were placed flat on the soil surface with the share resting under its self-weight near the soil surface, so that the plough initially experienced a large positive pitch (e.g. θ = 2-6°, depending on the initial skid settings), a shallow plough depth, D_{plough}, and a roll approximately equal to the slope angle ($\alpha = \beta$).

The DC motor (top left of Fig. 3a) was started which reeled in the line connected to a pulley which pulled the towing trolley horizontally along the top of the box. The plough then translated through the seabed whilst its position and the towing force required were logged continuously. When the trolley reached the end of its travel (after a plough movement, $\Delta x \approx 1200$ mm) the motor was stopped. Careful measurements were made of the final plough position and depth to confirm the measurement by the LVDT, DWT and inclinometers which was particularly important for the higher slope inclination where the plough moved away from the test box centreline.

On completion of the test and plough position measurements, the plough was removed from the seabed. Measurements of the seabed surface cross-section were taken every 250 mm along the travel path of the plough to find the position and depth of the trench and spoil heaps. This was done by

placing a rigid square section bar across the top of a test box to act as a reference height and then "dipping" down to the soil surface using a set of vernier callipers with a rear mounted dip meter modification. The accuracy of each of the measurements was approximately +- 1 mm. Each test was completed at least twice and average results for key output parameters calculated.

3. RESULTS: FLAT BED CASE

The result from the shallow depth testing for the flat seabed case ($\beta = 0°$) are presented initially to show typical plough behaviour and allow later comparison with the sloping seabed results (Figs. 4 and 5). Fig. 4a shows the plough depth and tow force variation as the plough is towed through the soil. Plough depth is defined as the vertical distance between the deepest part of the plough and the initial soil surface level. The plough starts with a small plough depth ($D_{plough} \approx 3$ mm) before movement of the plough (back of the share heel position, x = 31 mm). As soon as the plough moves the plough share starts to penetrate the seabed and the plough depth increases. After a movement of about 400 mm (20 m at prototype scale or 3.5 plough share lengths), the plough has reached a steady-state plough depth, D_{plough} = 21 mm (shallow depth case). Given that the plough is 1/50th scale, this corresponds to a prototype depth of 1.05 m. The tow force required to start the plough moving is approximately 4.7 N (588 kN at prototype scale) and this tow force increases until an average force of, F = 7.8 N (975 kN at prototype scale) when considered over the steady state plough depth. Greater average forces and depth were recorded for the medium depth flat seabed cases as shown in Table 1.

The kinematics of the plough are shown in Fig. 4b. The plough initially starts with a large positive pitch which then reduces to approximately -2° (-1° during medium depth ploughing) at steady-state conditions. At the same time, the plough roll (measured by the plough mounted inclinometer) fluctuates slightly with a mean value of $\alpha \approx 0.8°$. Fig. 4b also shows the plough depth and the trench depth, D_{trench} as measured manually following completion of the tests. It can be seen that D_{trench} is approximately 90% of D_{plough} which is thought to be due to local trench collapse and is similar to that observed by Lauder (2011). The trench role is the roll of the trench derived from manual measurements of the trench geometry following completion of the test.

Cross-sections of the trench and spoil heaps are shown in Fig. 5. The centre of the trench is at y = 250 mm (i.e. along the centre-line of the 500 mm-wide box) and the level of the base of the trench is 21 mm below the level of the original, flat seabed (so D_{trench} = 21 mm). Spoil heaps form on either side of the trench above the level of the original seabed. From the data shown in Fig. 5, the trench side-wall on the left hand side was found to be 31° to the horizontal and 29° to the horizontal on the right hand wall. Note that both of these angles are just below the critical state, $\phi'_{crit} = 32°$ and so are just stable.

When ploughing with no roll the share walls, which support the trench walls during ploughing, will be at 30° to the horizontal (i.e. so the full share blade angle = 180 – 2 x 30 = 120°). Given that one trench wall was slightly steeper than the other, these measurements suggest that the plough experienced a slight clockwise roll, α = (31-29)/2 = 1° consistent with the $\theta \approx 0.8°$ measured by the inclinometer (Fig. 4.).

4. RESULTS: ALL SLOPE ANGLES

4.1 Tow forces

Fig. 6 shows the measured relationship between tow force and plough movement for the tests with different slope angles ploughing at medium depth. The general response of each test shows an increasing tow force before steady-state towing conditions are reached. However, there seems to be a reduction in average tow force for the larger slope angles and this behaviour is compared in Fig. 7a and 7b with both trench depth and plough depth. The average tow force was determined by averaging the tow force in the steady state zone (typically between a plough position x between 600 and 800 mm) which was identified by constant plough depth. Each test case was repeated at least three times and the average of the results was then determined.

For shallower trenching (Fig. 7a) the tow force seems relatively unaffected by the increase in slope angles with similar being observed for plough depth until the extreme slope of 30° where there is a noticeable increase in plough depth. Similar plough depth response is noted for medium depth ploughing in Fig. 7b but the measured tow force is initially highest for the flat slope and 5° inclination before reducing between 10 and 15° inclination to 84% of that for the flat bed case. There is also a further reduction in tow force for the extreme 30° case which is associated with an increase in ploughing depth. What is noticeable though for both depth cases is the significant effect of plough and slope inclination on the constructed trench depth with significant reductions in trench depth occurring for slope angles above 5° in both cases, for shallow trenching this is of the order of 30% when moving from 5° to 10° slope inclination which then remains relatively constant with increasing slope inclination. For the medium depth case the reduction in depth occurs between 5 and 15° slope inclination but is more significant with a 60% reduction. What is noticeable though is that both final trench depths are similar irrespective of initial plough depth suggesting the initial slope geometry controls the final trench depth.

As tow force and plough depth are interrelated it is useful also to show results as a force depth relationship as shown in Fig. 8. The results for the various slope inclinations are shown compared to a flat case derived using the formula proposed by Cathie and Wintgens (2001) to predict ploughing tow forces:

$$F = C_W W' + C_S \gamma' D^3 \quad (1)$$

where C_w is the interface friction coefficient (measured as μ = tan 24^o = 0.445 in the sand-steel interface tests), W′ is the plough's buoyant self-weight, C_s represents a combined passive earth pressure coefficient and shaping factor for the particular plough which was taken as 12.2 for loose soil as recommended for revised C_s values determined by Lauder et al., (2013), γ' is the soil's saturated unit weight and D is the plough depth $D_{plough.}$

4.2 Plough kinematics and final trench geometry

The movement of the plough and the final geometry of the trench are discussed together because they are closely interlinked, particularly for shallow slope angles.

Figure 9 shows the variation of plough roll with slope angle for the shallow depth ploughing. The plough roll, α would be expected to be equal to the slope angle, β for all slope angles if the skids remain on the sloping surface of the soil throughout ploughing without penetrating the seabed and the plough does not yaw significantly. This appears to be approximately the case: a best fit line to the data suggests $\alpha = -0.4 + 0.96\beta$, where the -0.4° may be a calibration offset error, and the 4% reduction of the gradient might be due to yaw (see later discussion). It may be suitably accurate to simplify the relationship to $\alpha = \beta$ (dashed line in Fig. 9).

The measured trench cross-sections produced by the rolling plough (α) on inclined slopes (β) are shown in Fig. 10. For each slope condition, the horizontal position, y and vertical elevation, z are plotted. The figure shows: (i) that the trench 'rolls' with the slope angle; (ii) that there is a reducing sized spoil heap on the upslope side for larger slope angles, and; (iii) that the constructed trench migrates down-slope for larger β.

The behaviour is discussed in more detail by examining the results for a slope angle, β = 20° for medium depth ploughing as shown in Fig. 11 which shows the original ground cross-section and final trench cross-section alongside an indication of where the plough was during ploughing. The trench wall angles are first examined. The trench data reveals that the average right side slope angle = 10° and the left side slope angle = 32° along the length of the trench. The measured plough roll, α = 21° during the test implies a trench angle of 30-21= 9° on the down-slope side (based on a plough wall angle of 30° determined in the flat bed test) and an angle of 30 + 21 = 51° on up-slope side while supported by the plough (sketched approximately on Fig. 11). The final measured down-slope angle is in good agreement with the prediction based on the plough roll because the down-slope trench wall remains stable: its angle to the horizontal is less than ϕ'_{crit}. This holds true for any possible slope angle

and the relationship with slope angle is shown in Fig. 12 together with a dashed line showing that this angle ≈ 30 - α to the horizontal (shown as a negative angle for clarity in Fig. 12).

In contrast, the up-slope wall was not stable for the 20 degree slope because 30 + 21 = 51° > ϕ'_{crit}. Consequently, although the soil was partially supported by the plough when the plough was in the trench, the slope angle then degraded to ϕ'_{crit} and sand collapsed into the trench resulting in a reduction in trench depth. This was observed generally for all slope angles (Fig. 12). A spoil heap is sketched on the up-slope side of the trench in Fig. 11 alongside an indication of the position of the plough during trenching. The spoil heap size and position was deduced based on the assumption that the collapsed volume of soil supported by the plough, A_{tc}, will equal the new volume of soil left in the final trench once the plough has passed because the soil is at critical state, constant volume shearing conditions. Note that this suggests that there is a smaller up-slope spoil heap above the plough even when the plough is in place, as the soil is not totally supported by the plough because it can flow down the slope around it (i.e. out of the plane of Fig. 11).

As shown in Fig. 7 the final trench was clearly shallower than the plough depth because of the collapse of the up-slope trench wall. This is shown as trenching 'efficiency', D_{trench}/D_{plough} in Fig. 13 for the shallow and medium depth plough setting. As observed previously, for β > 10° the trench depth was markedly shallower than the plough depth ($D_{trench}/D_{plough} \leq 0.64$). There is limited reduction in efficiency on a slope of 5° as this results in an upslope trench wall (Fig. 12) that just exceeds the critical state friction angle (30 + β =35°), but when β > 10° reductions in final trench depth are significant due to trench wall collapse. Fig. 11 also indicates that the horizontal position of the final trench will differ to that of the centre of the plough share during ploughing due to collapse of the uphill trench wall.

As a consequence of the sloping seabed, the plough roll and the spoil movements the final spoil volumes on each side of the trench differ (Fig. 14a and 14b). Fig. 14 shows that the up-slope spoil heap reduced in volume with slope angle and no spoil heap at all was found for β ≥ 25°. In contrast, the down-slope spoil heap volume generally increased with slope angle as seen in Fig. 10. This will have consequences for backfilling of the trench. There is a notable reduction in down slope spoil volumes for the slope inclined at 30° which is likely to be as a result of the down slope itself failing and flow of soil over the down slope spoil heap making it difficult to determine the full downslope extent of the down slope spoil heap with β close to the critical state friction angle of the soil. Similar behaviour is observed for the two plough depths with Figs. 14a and 14b highlighting the potential for greater spoil production with increasing initial plough depth.

4.3 Down-slope plough movements

In addition to the changes in tow force and trench geometry, the plough had a tendency to move down-slope as it was being pulled. Fig. 15 shows a schematic plan view of the geometry of the towing point, the tow line and the plough. Although the tow point was fixed in the direction perpendicular to plough movement (the y-direction), the plough moved down-hill by an amount $\Delta y_{,plough}$ during ploughing, giving an out of plane tow angle, η. In addition, the plough yawed so that the skids were uphill of the share. Finally, because of up-slope trench collapse, the final trench was even further downhill than the plough position.

Fig. 16 shows the plan coordinates (x and y) of the measured trench centre-line for all slope angles during shallow ploughing. Although the trench started at coordinate (x = position of rear of each plough, y = 250 mm, i.e. left hand side of the box, at the centreline), the trench deviated down-slope before continuing along the slope with a deviation $\Delta y_{,trench}$, where $\Delta y_{,trench}$ increased with slope angle. When steady-state conditions were reached, the plough was traversing the slope with a fixed $\Delta y_{,plough}$.

Unfortunately, neither yaw, plough $\Delta y_{,plough}$ or tow angle, η were measured directly during testing. However, Fig. 17a and 17b shows the measured pitch, deduced tow angle, η and deduced yaw of the plough. Note that the calculation of η was based on measurement of final trench positions using $\eta=\sin^{-1}(\Delta y/L)$, where L is the tow wire length and $\Delta y_{,trench}$ the trench down-slope movement. Consequently, η will be overestimated because the trench centreline will be down-slope of the plough position (Fig. 15). The yaw, δ was estimated from the slope geometry assuming that $\delta=\sin^{-1}(\tan\theta/\tan\beta)$. This assumes that the additional negative plough pitch on a slope was entirely a consequence of the difference in elevation of each end of the plough as the share was below the skids because of yaw. The results confirm that the yaw, pitch and down-slope movements were significant for large slope angles. Fig. 17a and 17b show that for shallow ploughing there is greater potential for down slope movement ($\Delta y_{,plough}$) resulting in an increased out of plane tow angle. Although the yaw angles were normalised for the initial increased pitch for the shallow ploughing skid settings there also seems to be greater potential for yaw during shallow ploughing.

5. DISCUSSION AND IMPLICATIONS FOR PRACTICE

Despite the very high slope angles approaching the soil's angle of friction, the plough remained stable. The plough roll was found to be approximately equal to the slope angle (roll, $\alpha \approx$ slope angle, β). This implies that the skids remain flat on the inclined soil surface and that the ploughing operation itself is possible. Unfortunately, although the plough is stable the plough runs parallel to the towing point but offset down the slope so that there is an out of plane towing angle (η) which increases with steepness of the slope and becomes more significant at slope inclinations of above 10° to 20° depending on the depth of ploughing. For example, the prototype trench offset for medium depth ploughing increases from 1.6 m on a slope inclined at 20° to 4.8 m on a slope inclined at 30°. At the

same time, the plough will yaw so that trench share centre is downhill from the towing point (again increasing with β). The yaw may be a more significant consideration for pre-layed pipelines where the pipeline is first placed on the seabed, the plough then lifts the pipeline up into its body, and the pipeline passes through the plough during ploughing. The pipeline itself has limitations on the bending stresses that may be induced during this process (to avoid pipeline damage) and the plough monitors internal pipeline rollers to limit these stresses. The results suggest that if the pipeline is prelayed in the predicted downslope position the plough yaw may be up to 12° (Fig. 17b) with this angle fixed over the 16.85 m length of the plough. Both the down slope movement and yaw may be managed to some extent as real offshore ploughs have active skid height and steering capabilities (e.g. the DeepOcean APP plough can steer to an angle of 7° either side of straight ahead), but otherwise would need to be considered in route optimisation, particularly if there were frequent changes in slope angle.

Although it is often assumed that encountering a geohazard will affect the tow force, it is the authors' experience for model ploughs (where plough skid settings which control initial depth are fixed during testing) that tow force is relatively unaffected by changes in seabed conditions, instead it is the depth of trenching that changes. For example, in dense sand the plough will trench shallower than in loose sand (Lauder, 2011) whilst maintaining a relatively constant tow force. This response is referred to as the 'long-beam' principle (Palmer, 1999). Therefore, the lack of significant change in tow force with slope inclination angle in shown Figs. 7a and 7b is unsurprising. The tow force reduced with increasing slope angle to a moderate degree in the medium depth ploughing (Fig. 7b and Fig. 8), with very little change in plough depth until reaching a slope inclination of 30° where there was notable increase in plough depth for both initial plough depth settings. More detailed inspection of the behaviour is shown in Fig. 8 which shows that on inclined slopes the tow force-depth relationship tends to fall slightly below the values predicted by Eq. (1) with increasing slope inclination suggesting that the increase in slope angle may be influencing the components of passive resistance that contribute to the C_s term. It also serves to highlight the significant change in behaviour when the slope reaches 30° which may be as a result of the non-linear reduction in factor of safety against slope failure (ratio of resisting shear stress to those tangentially down the slope) which occurs as the slope angle approaches the critical state friction angle of the soil (ϕ'_{crit}). For instance, if the slope is considered as a simple dry infinite slope the factor of safety can be estimated from the ratio of $\tan\phi'_{crit}/\tan\beta$ therefore for a slope of 5° the factor of safety would be 7.1 whereas at 30° this falls to 1.08 and is just stable prior to disturbance by the plough. Therefore, for soil deformation which is symmetric about the plough centreline axis, the increase of work required to move soil on the up-slope side of the plough is likely to be offset by the reduction on the down-slope side. Furthermore, any soil deformation mechanism would be expected to bias towards the down-slope movement which would give a net reduction in overall work moving the soil (and therefore tow force).

What would seem to be apparent from the investigation is that the behaviour of the plough itself is not the limiting factor (depth and tow forces relatively unaffected at lower slope inclinations) on operations but the potential for up-slope trench wall collapse resulting in significant loss of final trench depth (Figs. 7a, 7b and 13). The down-slope trench wall is formed at an angle of approximately 30-β to the horizontal (for the plough geometry used here). It remains at this angle after the plough passes, because intrinsically stable. In contrast, the up slope trench wall is at 30+β when the plough is in place (Fig. 12). Consequently, the wall will eventually collapse to an angle of ϕ'_{crit} resulting in the observed reduction in the trench depth (Fig. 13), reducing the size (or eliminating) the uphill spoil heap (Figs. 17a and 17b) and moving the centre-line of the final trench down-slope. The consequences of the up-slope trench wall collapse for the pipeline depends on how the pipeline is laid. If the soil falls back into trench before the pipeline is placed into the trench (e.g. if the pipeline is post-laid, or if the zone of collapse is in the pipeline free-span or lay-back length behind the plough) the pipeline will rest on the final trench profile, giving a reduced trench depth and the potential for localised "out of straightness". Alternatively, if the pipeline is placed into the base of the trench before the up-slope wall collapses (i.e. because the duration of the pipeline in the lay-back length is shorter than the time that the trench wall is stable), this may achieve partial burial of pipeline before any engineered backfilling and increase the final cover depth. However, for this latter case, the potential for asymmetric backflow conditions should be considered as it may generate bending stresses within the pipeline.

The results also highlight that any backfilling operation may be significantly affected by the increasing slope inclination (Fig. 14). The uphill spoil heap will be much smaller than that on the down-slope side (and may not exist for $\beta \geq 15$-$20°$) and the down slope spoil heap will be enlarged. If a mechanical backfill plough is used, which is assumed initially to run level with the slope (i.e. have $\alpha = \beta$), the achievable cover depth will be limited and asymmetric with transient asymmetric backfill forces applied to both the pipeline and the plough. The latter may make backfill ploughing operations impractical requiring backfilling operations using separately sourced borrow material or rock dump.

The findings of the laboratory investigation generally supports the current anecdotal guidance that suggests that cross slope ploughing on slopes up to 5º does not pose any significant risk to operations. However, this appears sensitive to both the plough geometry (and consequently the geometry of the trench formed) and the critical state friction angle of the soil. Therefore, in a soil with reduced friction angle and/or when using narrow plough share this guidance may not be conservative. However, the study suggests that ploughing is possible at greater slope angles but that the risks to ploughing and backfilling operations will increase at slope inclination angles of 10° and above (as the stability of the slope reduces). Given the specific geotechnical conditions studied herein (loose drained siliceous

sand), this finding is not generalisable and site-specific assessment of trench operations should be performed before ploughing across significant seabed slopes.

6. CONCLUSIONS

A series of laboratory model tests were conducted to investigate the performance of pipeline ploughs on sand slopes. For the conditions tested, the tests revealed that although the model plough could operate up to slope inclinations of 30° the depth of the final trench formed was severely reduced due to trench collapse at slopes inclined at 10° or steeper, whereas plough tow forces and depth were relatively unaffected. Where trench collapse occurs prior to pipeline touch down this would result in the pipeline being buried too shallow and out of specification. In addition, the position of the trench created by the model plough had a tendency to move down the slope to a steady state down-slope offset position, Δy, which depended on slope angle and depth of ploughing. In turn this behaviour was associated with yaw of the plough relative to the direction of progress which may lead to lateral loads on the pipeline and potentially damage to the pipeline or the plough. This may be managed to some extent as real offshore ploughs have active skid height and steering capabilities, but otherwise would need to be considered in terms of route optimisation and pipeline integrity, particularly if there were frequent changes in slope angle (e.g. in a sandwave field).

The spoil heaps normally used to backfill the trench became asymmetric with increasing slope angle with up-slope spoil heaps being no longer apparent due to up-slope trench wall collapse at slope angles above 15-20° with a consequent increase in the volume of available down slope spoil heap material. This may render backfill ploughing difficult or impractical due to the lack of spoil and asymmetry of the spoil available.

Current anecdotal guidance suggests that cross slope ploughing on slopes up to 5° does not pose any significant risk to operations and this is generally confirmed by this study. However, the model test results suggest that the effect of seabed slope will depend on both the plough geometry and the friction angle of the soil. Pipeline ploughing appears to possible at greater slope angles but the risks to ploughing and backfilling operations will increase at slope inclination angles of 10° and above which will limit the maximum slope angle which can be considered for real full scale operation. This suggests that where ploughing operations traverse slopes at any significant inclination a geotechnical study to assess the risks to operations should be performed.

REFERENCES

Allan, P.G., 2000. Cable security in sandwaves. In: Proceedings of the International Cable Protection Committee Plenary Meeting, Copenhagen, May 2000.

Bransby, M.F., Brown, M.J., Hatherley, A.J., Lauder, K.D. 2010. Pipeline plough performance in sand-waves. Part 1: model testing. Can Geotech J. 47 (2010), 49- 64. http://dx.doi.org/10.1139/T09-077.

Bransby, M.F., Yun, G., Morrow, D.R., Brunning, P., 2005. The performance of pipeline ploughs in layered soils, In Gourvenec, S., and Cassidy, M. (Eds.) 1st International Symposium on Frontiers in Offshore Geotechnics (ISFOG 2005), Perth, Western Australia, 2005, pp. 597-606

Brown, M.J., Bransby, M.F., Simon Soberon, F. 2006. The influence of soil properties on ploughing speed for offshore pipeline installation. In: Ng, C.W.W., Zhang, L.M. & Wang Y.H. (Eds.) 6th International Conference on Physical Modelling in Geotechnics (ICPMG'06), Hong Kong, China, 4-6th August 2006, pp. 709-714.

Cathie, D.N., Barras, S., Machin, J., 1998. Backfilling pipelines: State of the Art. In: Proceedings of the 21st Offshore Pipeline Technology Conference, IBC, Oslo, Norway, 1998.

Cathie, D.N., Wintgens, J.F., 2001. Pipeline trenching using plows: Performance and geotechnical hazards. In: Proceedings of the Thirty-third Annual Offshore Technology Conference, Houston, Texas, 30 April – 3 May 2001. 2001, pp. 1-14.

Cathie, D.N., Jaeck, C., Ballard, J.C., Wintgens, J.F., 2005. Pipeline geotechnics: state of the art. In Gourvenec, S., and Cassidy, M. (Eds.) 1st International Symposium on Frontiers in Offshore Geotechnics (ISFOG 2005), Perth, Western Australia, 2005, pp. 95–114.

Chen, Z., Liu, Y., Liu P., Bijker, R., 2001. An integrated approach to pipeline design through sandwave fields: Dongfang pipeline. In: Proceedings of OMAE 2001: 20th International Conference on Offshore Mechanics and Arctic Engineering, Rio de Janeiro, Brazil, 3-8 June 2001.

Cortis, M., Coombs, W.M., Augarde, C.E., Robinson, S., Brown, M.J., Brennan, A., 2017. Modelling seabed ploughing using the material point method. 1st International Conference on the Material Point Method for Modelling Large Deformation and Soil–Water–Structure Interaction, MPM 2017, 10 – 13 January 2017, Delft, The Netherlands. Procedia Engineering, 175 (2017). 1-7. DOI: 10.1016/j.proeng.2017.01.002.

Grinsted, T.W., 1985. Earthmoving in submerged sands, Ph.D. thesis, University of Newcastle upon Tyne, UK, 1985.

Lauder, K.D., Brown, M.J., Bransby M.F., Gooding, S., 2012. Variation of tow force with velocity during offshore ploughing in granular materials. Can. Geotech. J. 49.1244–1255. DOI: 10.1139/t2012-086.

Lauder, K.D., Brown, M.J., Bransby, M.F., Boyes, S., 2013. The influence of incorporating a forecutter on the performance of offshore pipeline ploughs. Applied Ocean Res. J. 39. 121–130. DOI: 10.1016/j.apor.2012.11.001

Lauder, K., Brown, M.J., 2014. Scaling effects in the 1g modelling of offshore pipeline ploughs. In: Gaudin, C. and White, D. (Eds.) 8th International Conference On Physical Modelling in Geotechnics (ICPMG'14), Perth, Western Australia, 14-17th January 2014. pp. 377-383.

Lauder, K.D., 2011. The performance of pipeline ploughs. PhD Thesis, University of Dundee, Dundee, UK.

Machin, J., 1995. Operational experience of multipass plough and backfill plough. In: Proceedings of the International Conference SUBTECH 95. 7–9 November 1995, Society of Underwater Technology, Aberdeen, UK, pp. 237–248.

Morrow, D.R., Larkin, P.D., 2007. The challenges of pipeline burial. In: Proceedings of the 7th International Offshore and Polar Engineering Conference. 1–6 July 2007, International Society of Offshore and Polar Engineers, Lisbon, Portugal, 2, pp. 900–907.

Palmer, A.C., 1999, Speed effects in cutting and ploughing, Géotechnique 49. 285-294.

Palmer, A.C., Kenny, J.P., Perera, M.R., Reece A.R., 1979. Design and operation of an underwater pipeline trenching plough, Géotechnique 29. 305-322.

Peng, W., Bransby, M.F. 2010. Numerical modelling of soil around offshore pipeline plough shares. In Gourvenec, S. and White, D. (Eds.) Proceedings of the 2nd International Symposium on Frontiers in Offshore Geotechnics: Frontiers in Offshore Geotechnics II, October 4, 2010, Perth, Western Australia, pp. 877-882.

Reece, A.R., Grinsted, T.W., 1986. Soil mechanics of submarine ploughs, In Proceedings of the Eighteenth Annual Offshore Technology Conference, Houston, Texas, 1986, pp. 453-461.

Wang, L., Gong, H., Xing, X., Yuan, J., 2015. Rigid dynamic performance simulation of an offshore pipeline plough. Ocean Engineering Journal 94: 51-66.

LIST OF SYMBOLS

D_{trench}	Trench depth
D_{plough}	Plough depth
F	Tow force
L	Tow wire length
V_{sup}	Spoil heap volume up-slope
V_{sdown}	Spoil heave volume down-slope
V_t	Trench volume
A_{tc}	volume of collapsed soil into trench
x	Horizontal position along trench line
y	Horizontal position perpendicular to trench axis
Δy	Down-slope plough or trench movement
Z	elevation compared to the box base.
α	Plough Roll
β	slope angle
δ	Plough yaw
η	out of plane tow angle
θ	Plough pitch

Figure Caption List

Fig. 1. The geometry of the trench and slope

Fig. 2. Schematic of the model plough geometry. Dimensions in mm.

Fig. 3. The experimental apparatus. (a) Schematic of the overall apparatus; (b) Image of plough from behind during testing.

Fig. 4. Test results for a flat seabed ($\beta = 0$) during shallow depth ploughing. (a) Tow force and plough depth; (b) Pitch and trench depth

Fig. 5. Example of the measured trench cross-section for the flat bed case (shallow ploughing).

Fig. 6. Tow force – displacement results for all slope inclinations (medium depth ploughing).

Fig. 7a. Variation of average tow force and trench depth with slope angle (shallow ploughing).

Fig. 7b. Variation of average tow force and trench depth with slope angle (medium depth ploughing).

Fig. 8. Relationship between average tow force and trench depth for all slope inclination angles.

Fig. 9. Plough roll angle against slope angle (shallow ploughing).

Fig. 10. Measured post-ploughed trench profiles (shallow ploughing).

Fig. 11. Trench cross-section and deduced plough position for the 20° slope (medium depth ploughing).

Fig. 12. Measured post-ploughing trench wall angles compared to values expected during ploughing (medium depth ploughing).

Fig. 13. Trenching efficiency variation with slope inclination.

Fig. 14a. Spoil volume characteristics for different slope inclinations (shallow ploughing).

Fig. 14b. Spoil volume characteristics for different slope inclinations (medium depth ploughing).

Fig. 15. Schematic plan view of trenching geometry. Note: all angles exaggerated for clarity.

Fig. 16. Plan view of measured final trench position for all slope angles (shallow ploughing).

Fig. 17a. Pitch, yaw and tow angle variation with slope inclination (shallow ploughing).

Fig. 17b. Pitch, yaw and tow angle variation with slope inclination (medium depth ploughing).

Table Caption List

Table 1. Slope test conditions and average results obtained for shallow depth ploughing conditions.

Table 2. Slope test conditions and average results obtained for medium depth ploughing conditions.

Fig. 1. The geometry of the trench and slope

Click here to download high resolution image

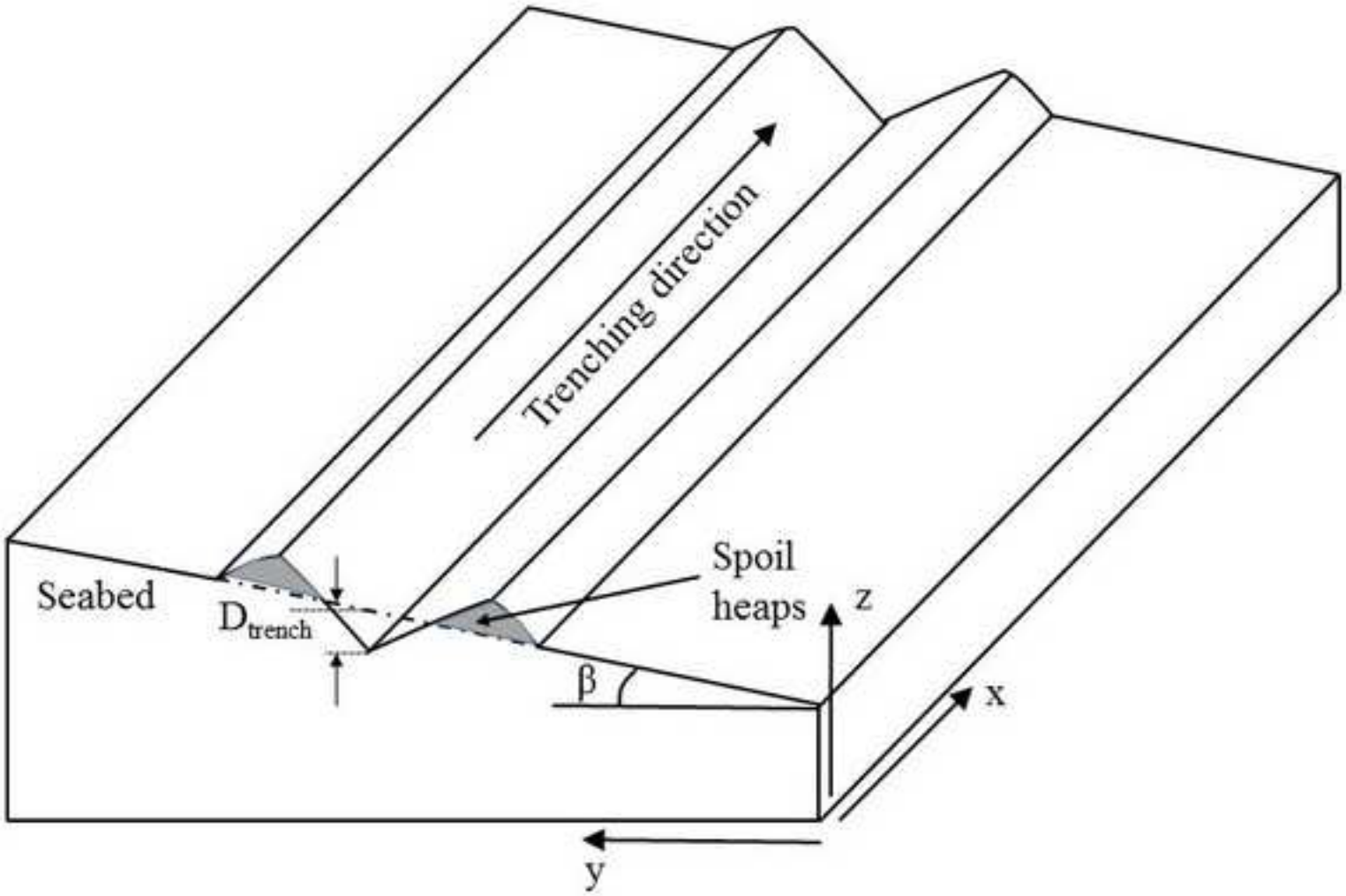

Fig. 2. Schematic of the model plough geometry. Dimensions in mm

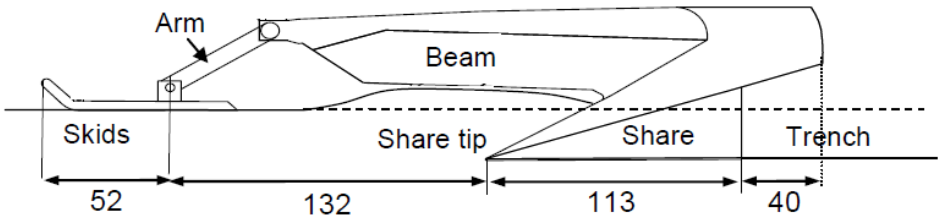

(a) Elevation

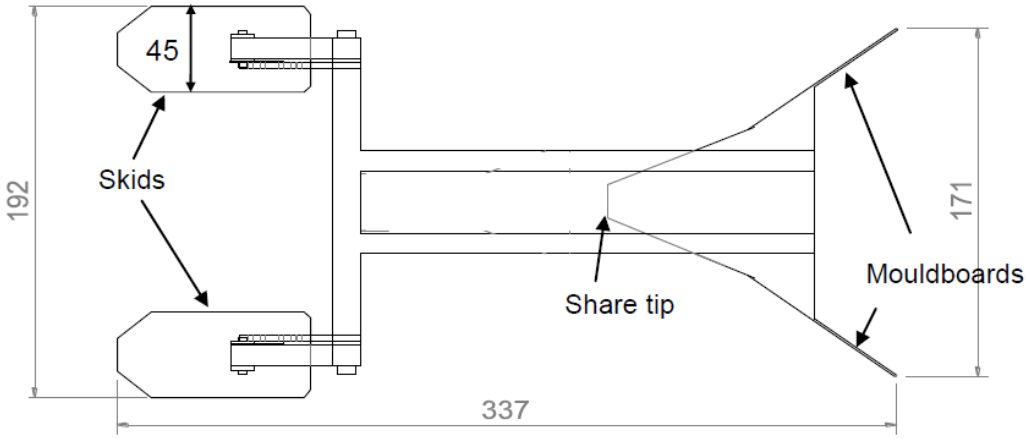

(b) Plan view

Fig. 3. The experimental apparatus. (a) Schematic of the overall

Click here to download high resolution image

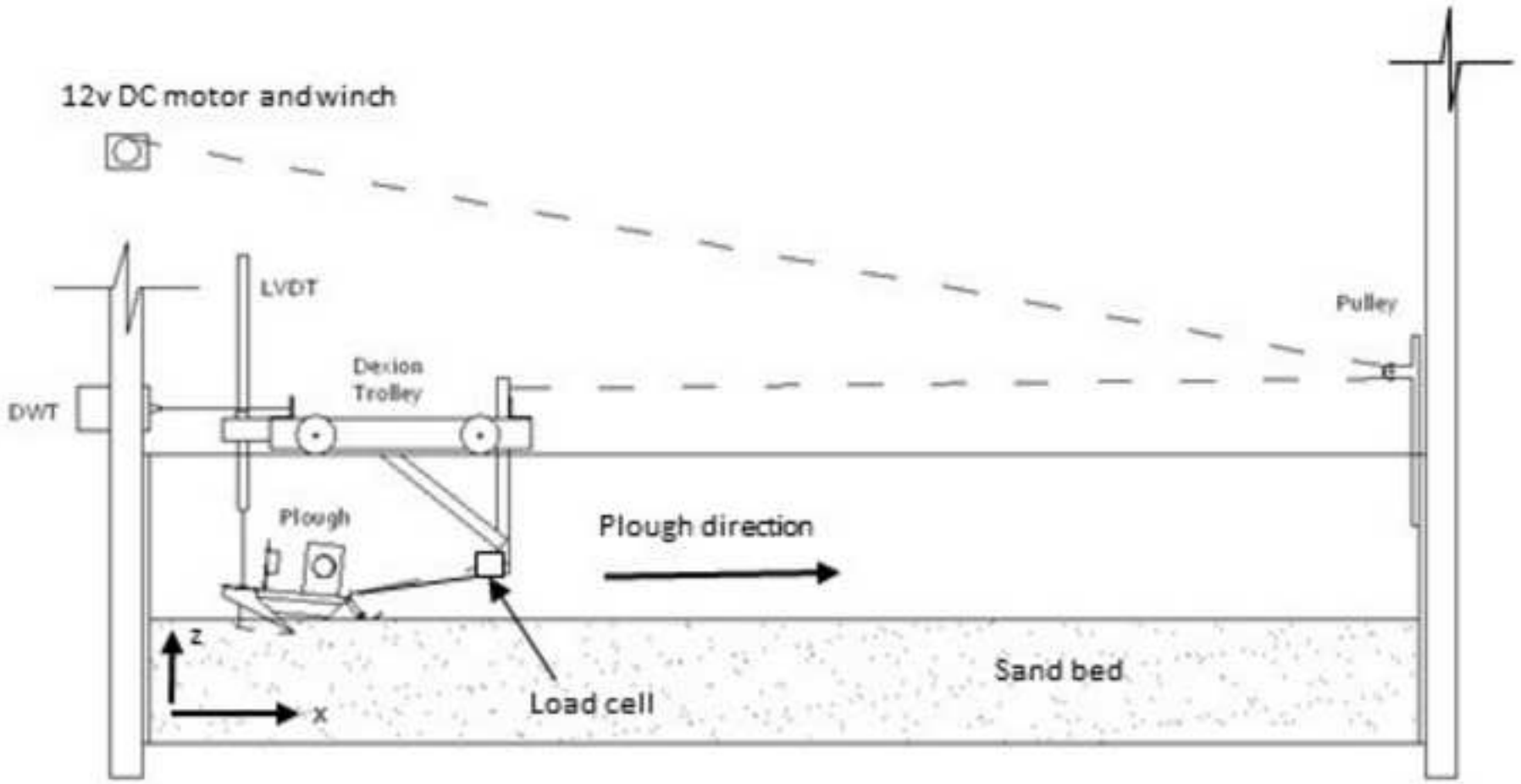

Fig. 3. The experimental apparatus. (b) Image of plough from be

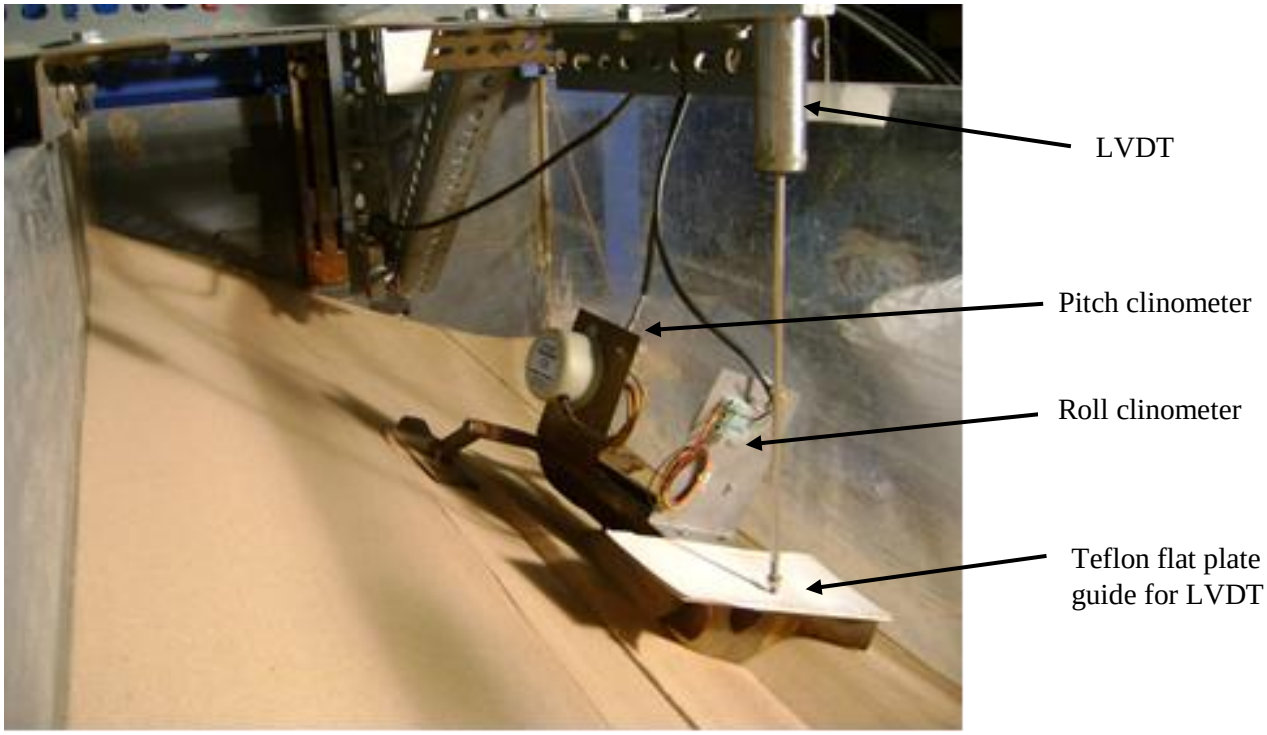

Fig. 4. Test results for a flat seabed (B = 0) during shallow de

Click here to download high resolution image

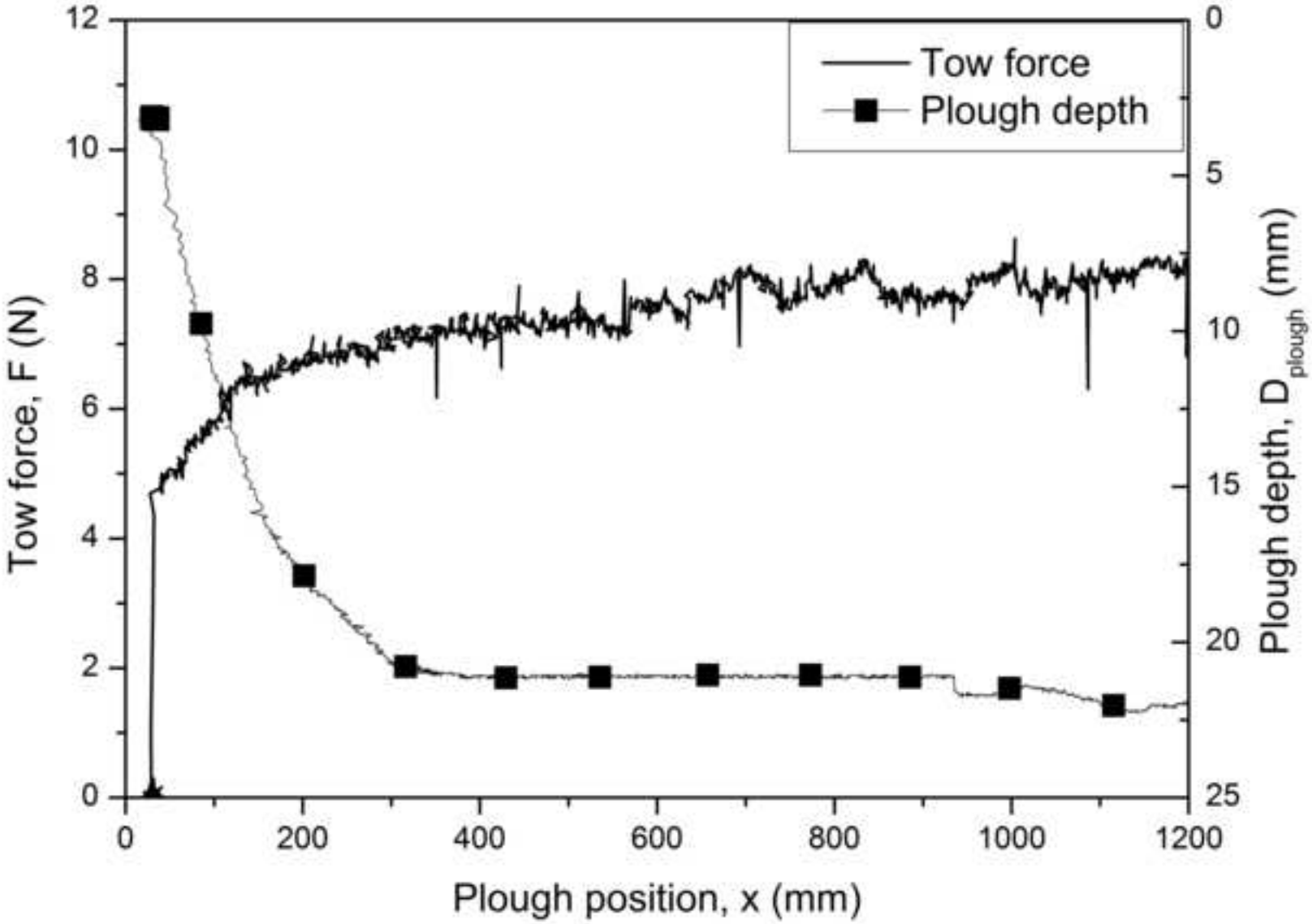

Fig. 4. Test results for a flat seabed (b = 0) during shallow de

Click here to download high resolution image

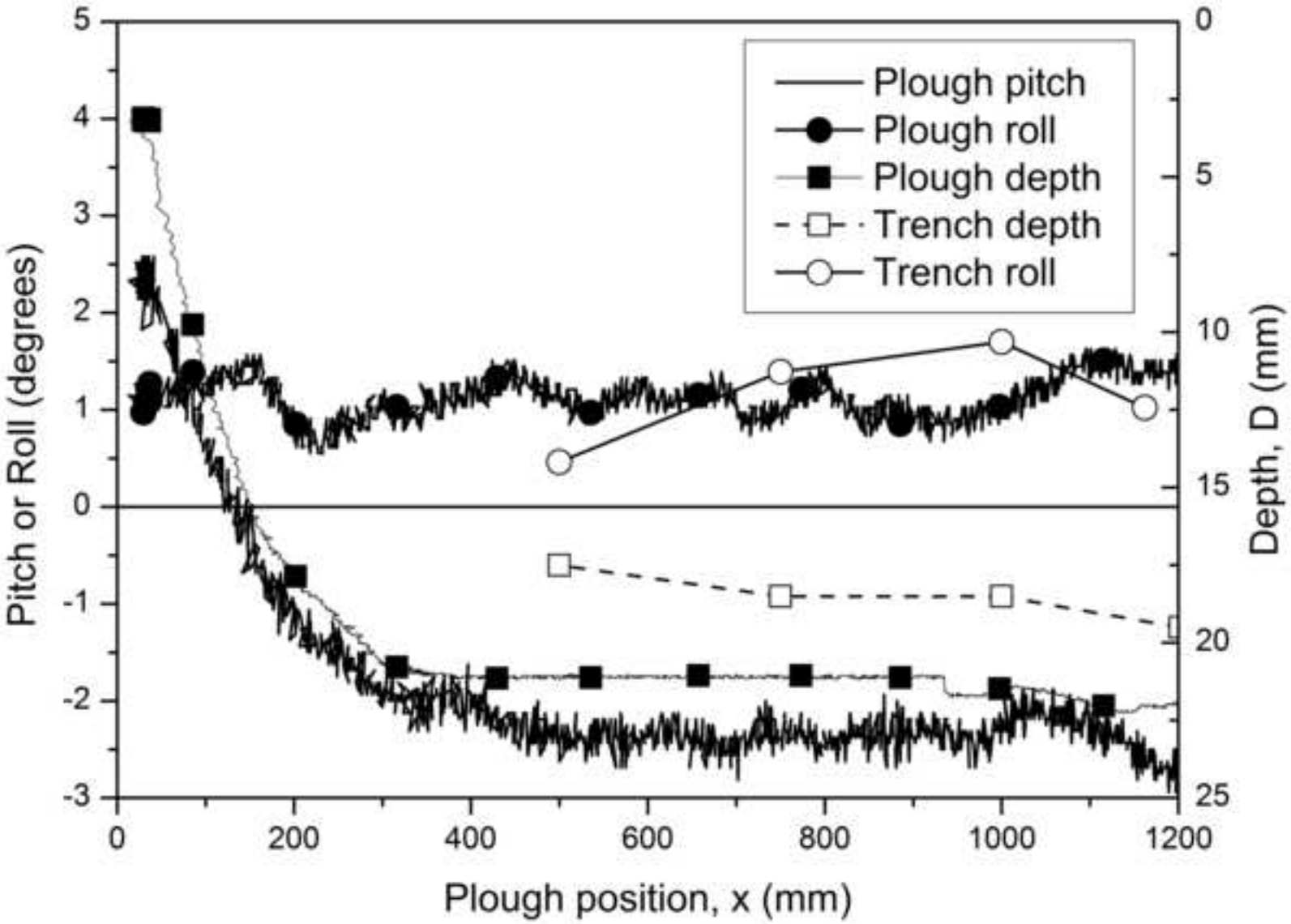

Fig. 5. Example of the measured trench cross-section for the fla

Click here to download high resolution image

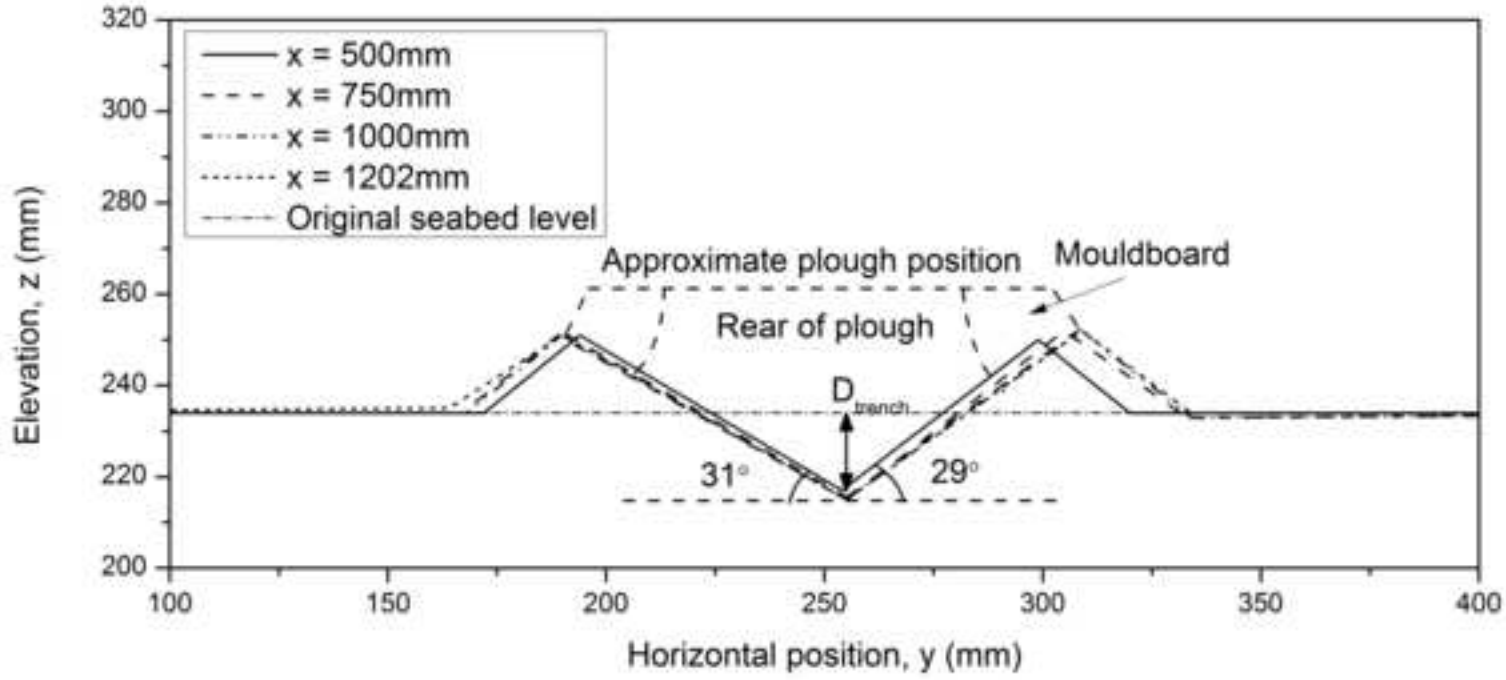

Fig. 6. Tow force - displacement results for all slope inclinati

Click here to download high resolution image

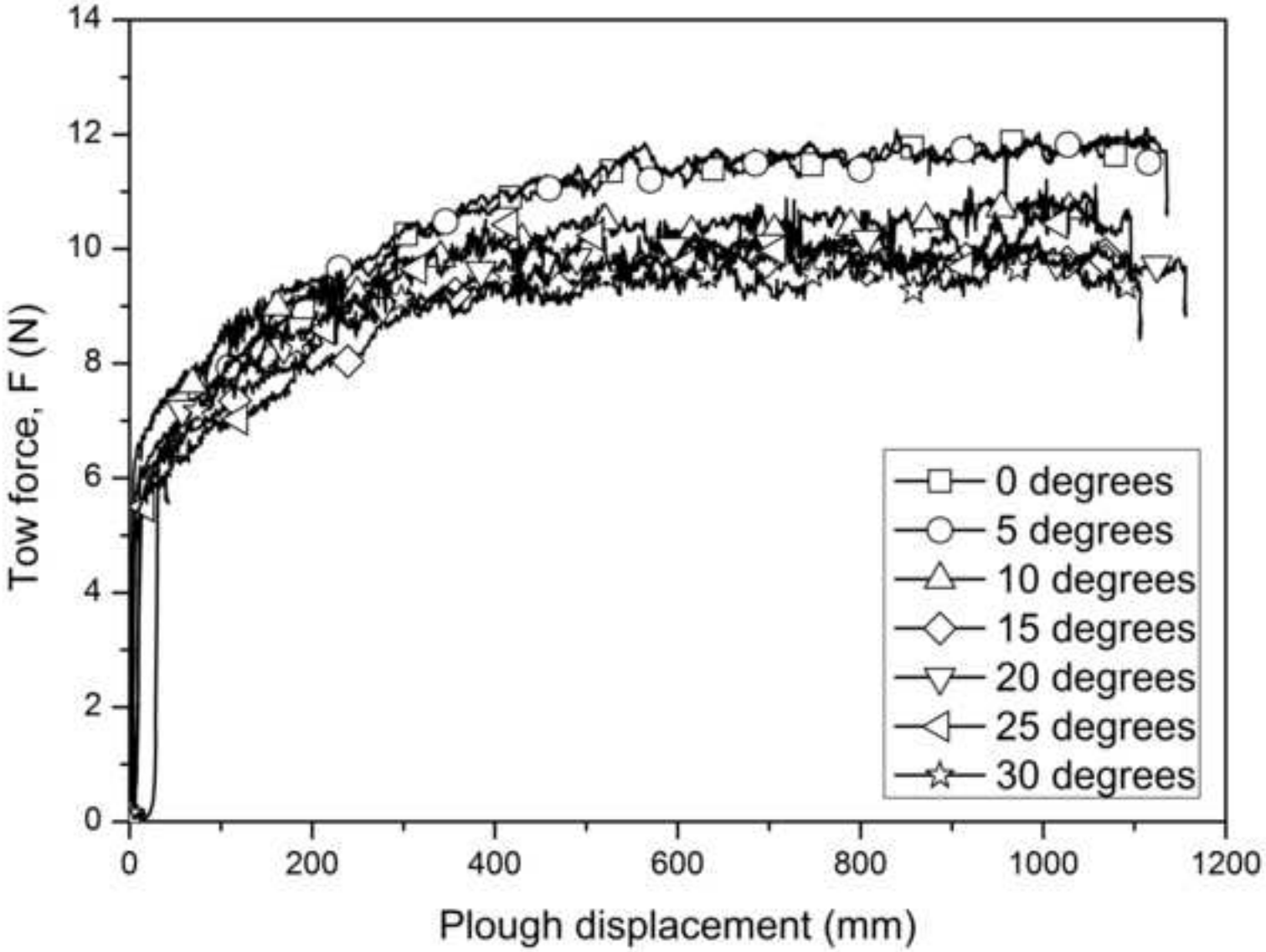

Fig. 7a. Variation of average tow force and trench depth with sl

Click here to download high resolution image

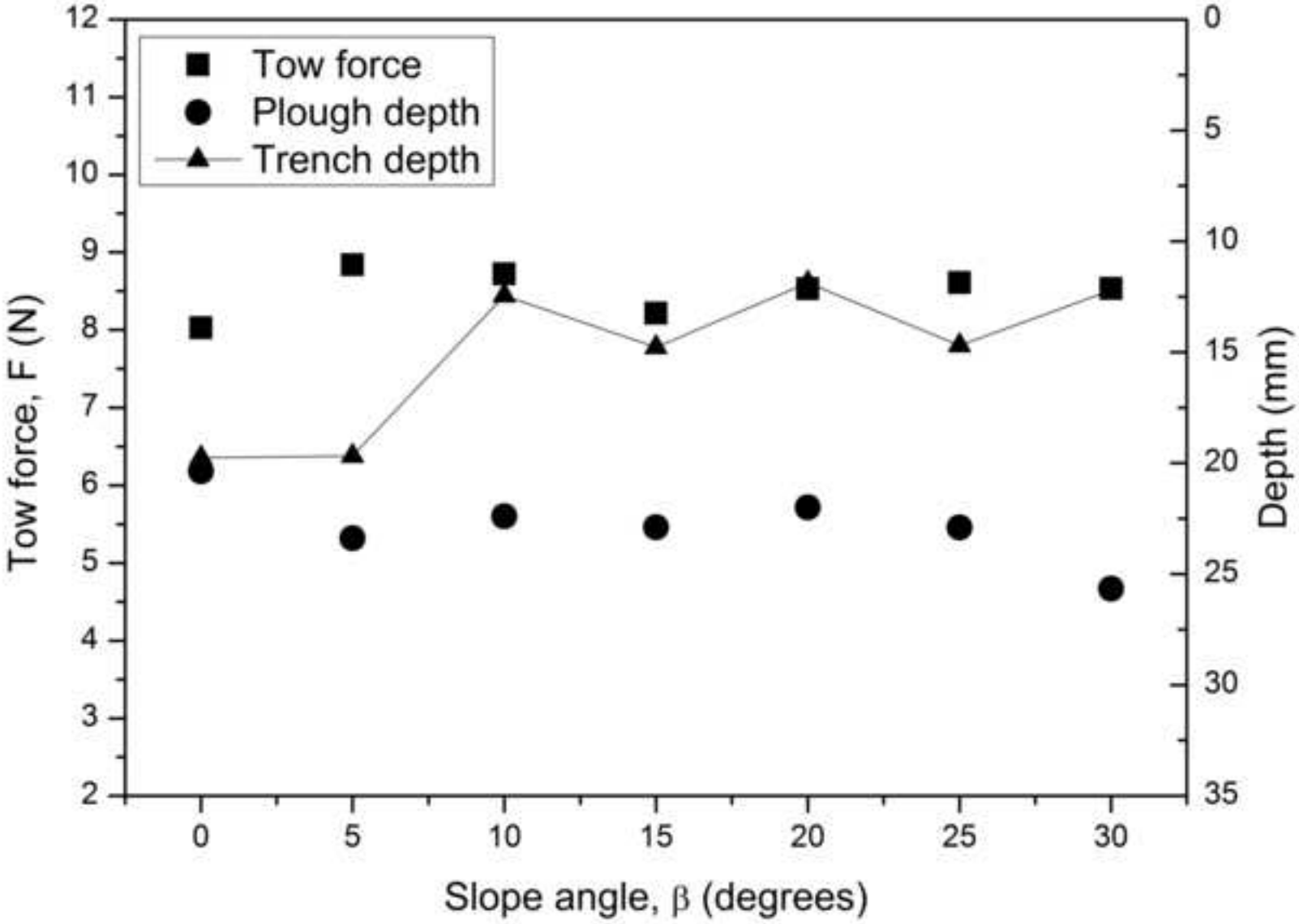

Fig. 7b. Variation of average tow force and trench depth with sl

Click here to download high resolution image

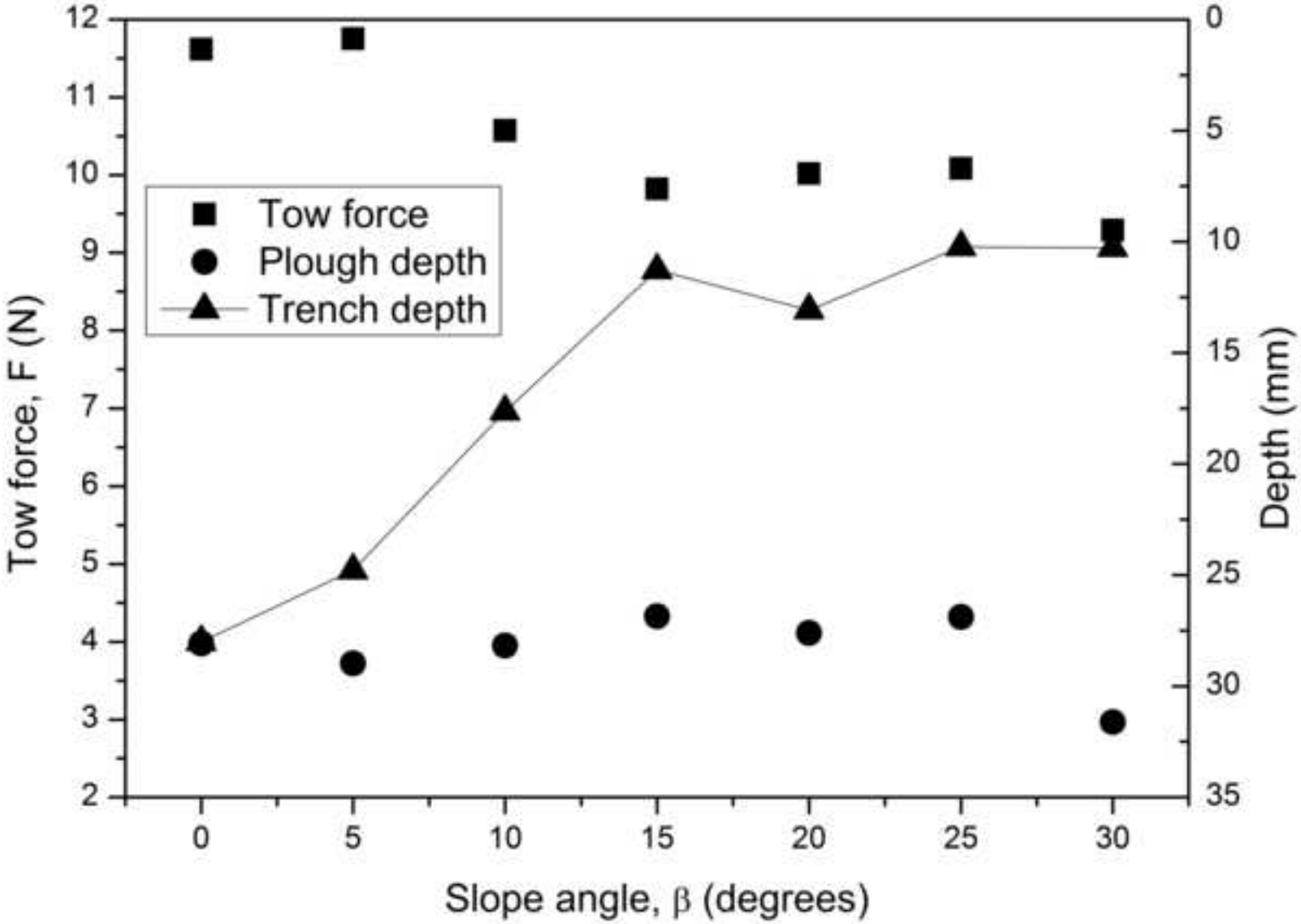

Fig. 9. Plough roll angle against slope angle (shallow ploughing

Click here to download high resolution image

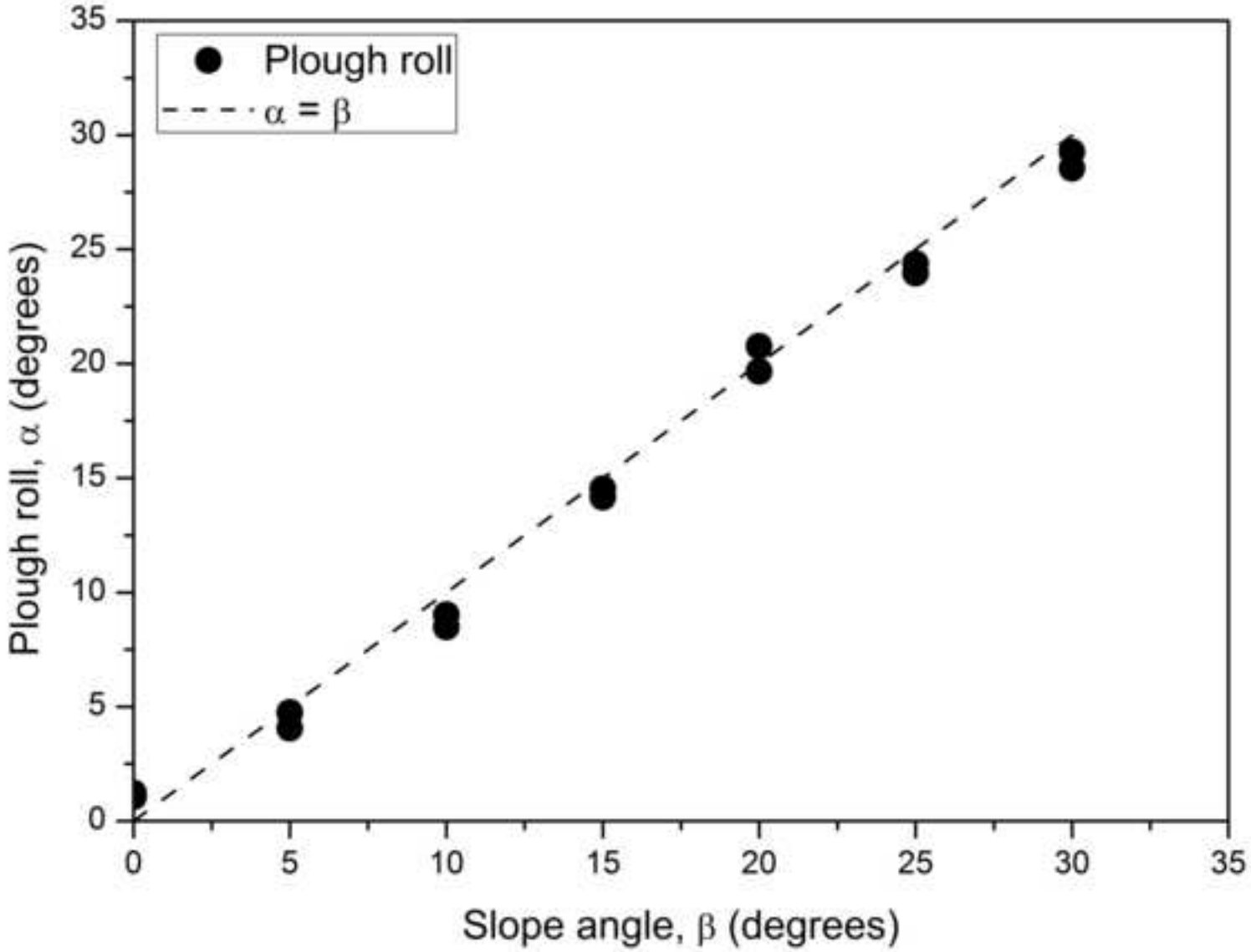

Fig. 10. Measured post-ploughed trench profiles (shallow ploughi

Click here to download high resolution image

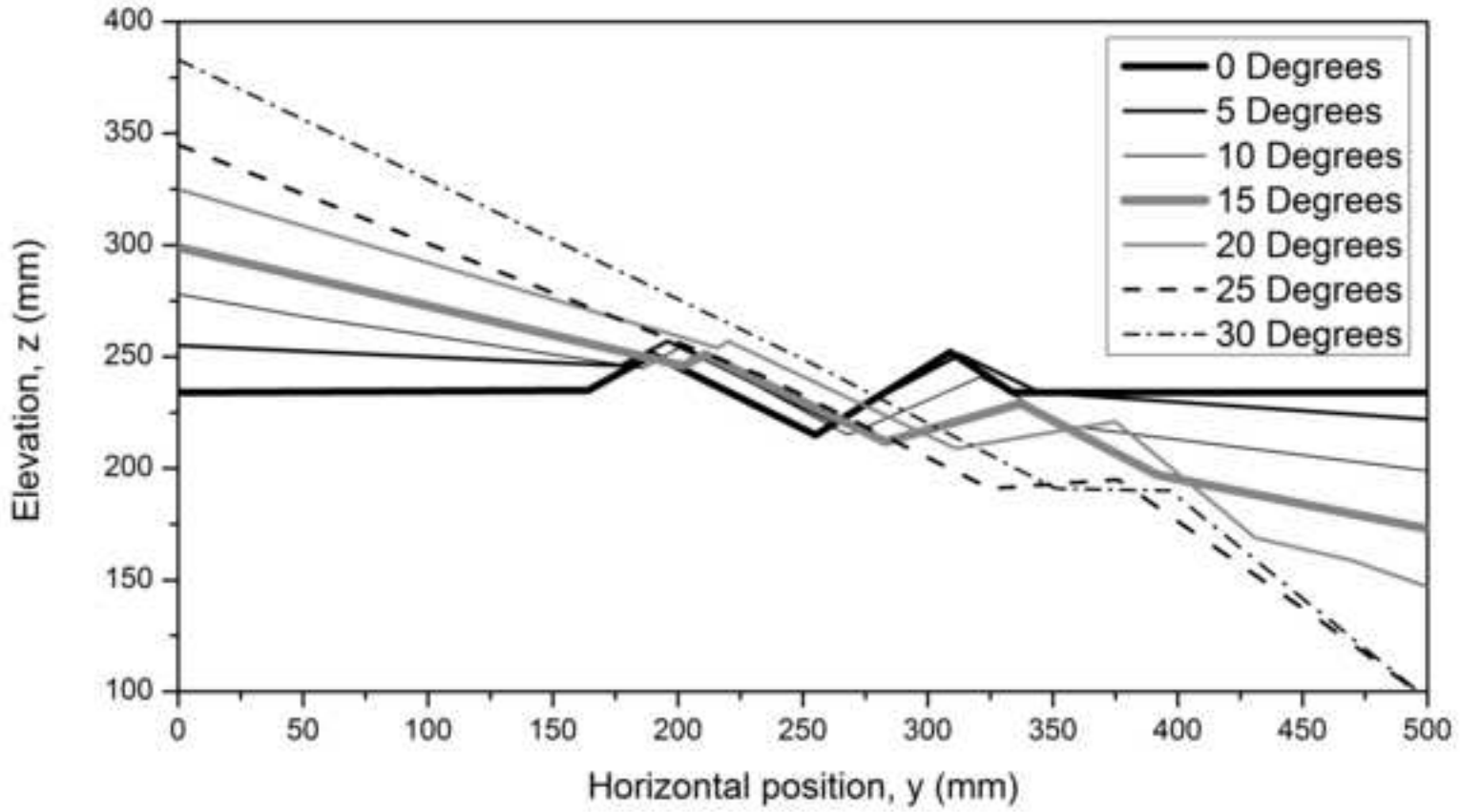

Fig. 11. Trench cross-section and deduced plough position for th

Click here to download high resolution image

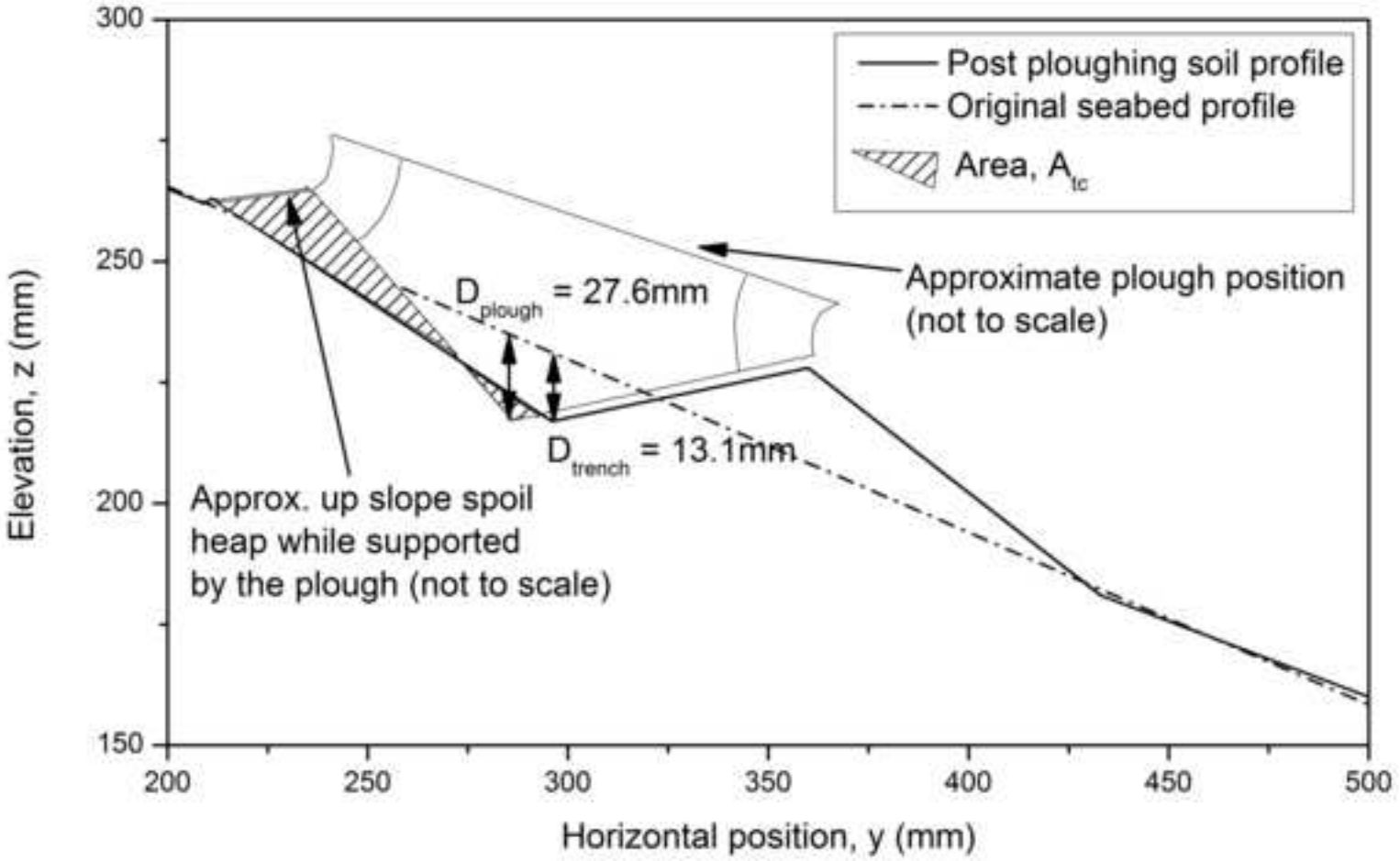

Fig. 12. Measured post-ploughing trench wall angles compared to
Click here to download high resolution image

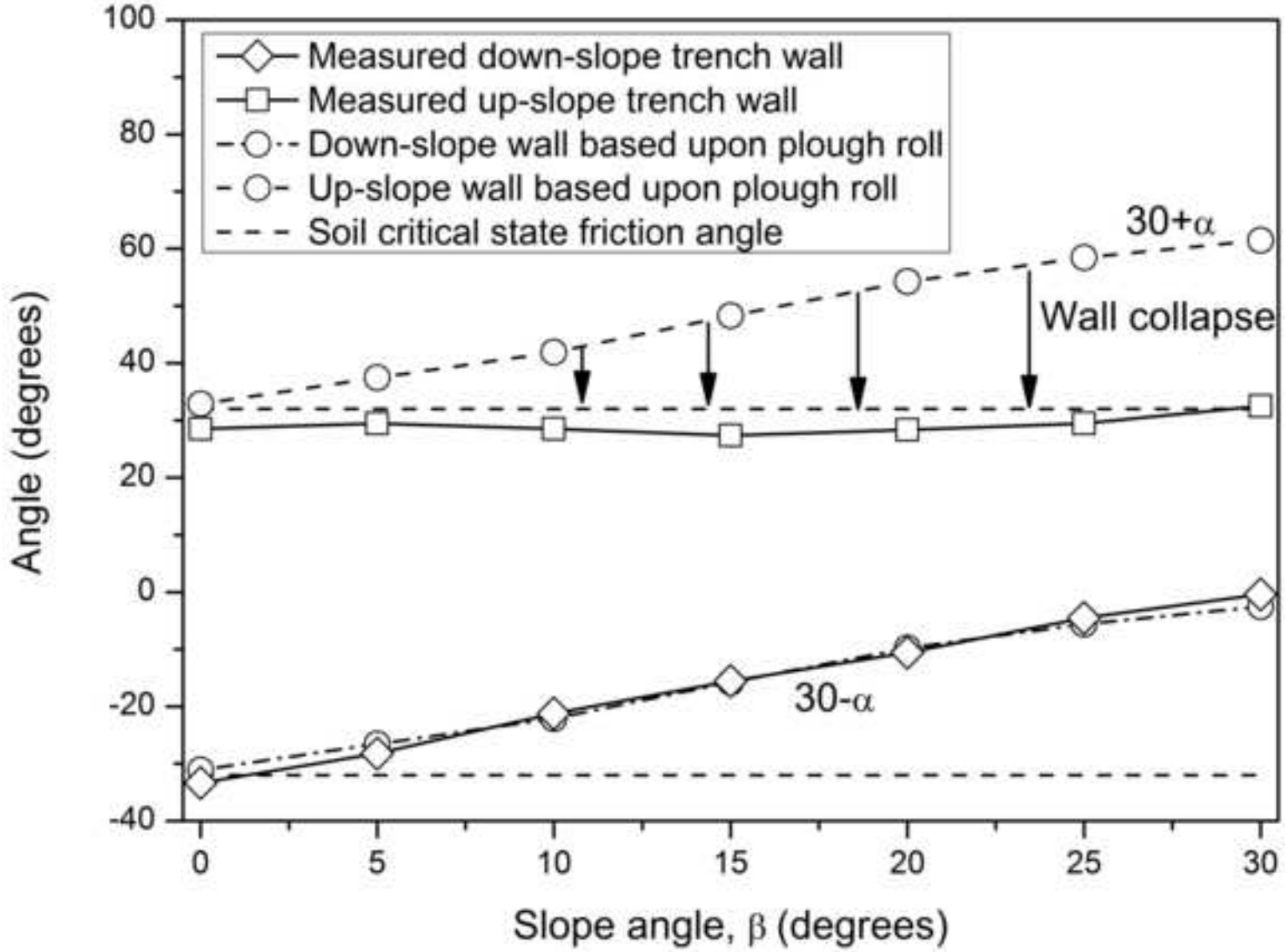

Fig. 13. Trenching efficiency variation with slope inclination.
Click here to download high resolution image

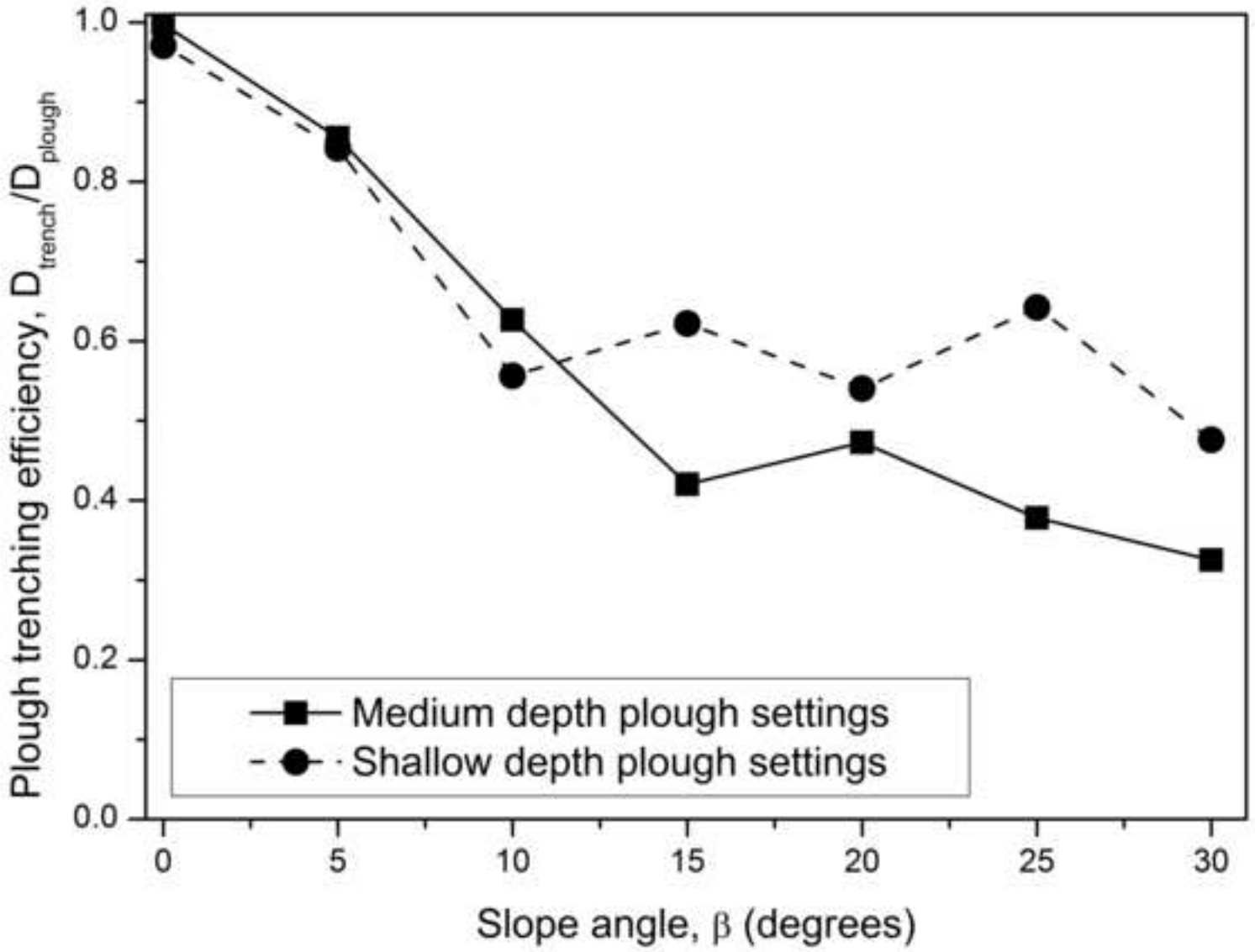

Fig. 14a. Spoil volume characteristics for different slope incli

Click here to download high resolution image

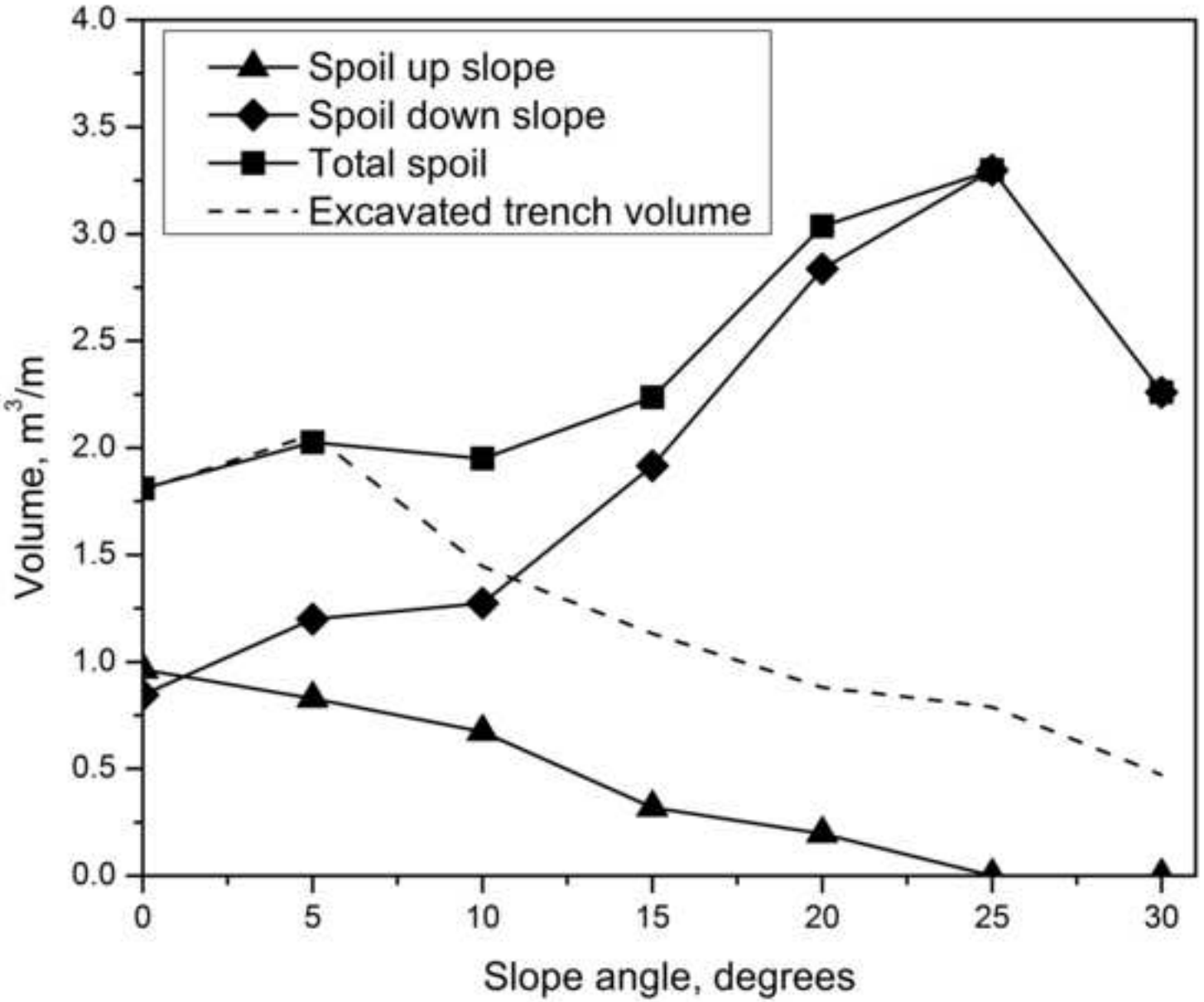

Fig. 14b. Spoil volume characteristics for different slope incli

Click here to download high resolution image

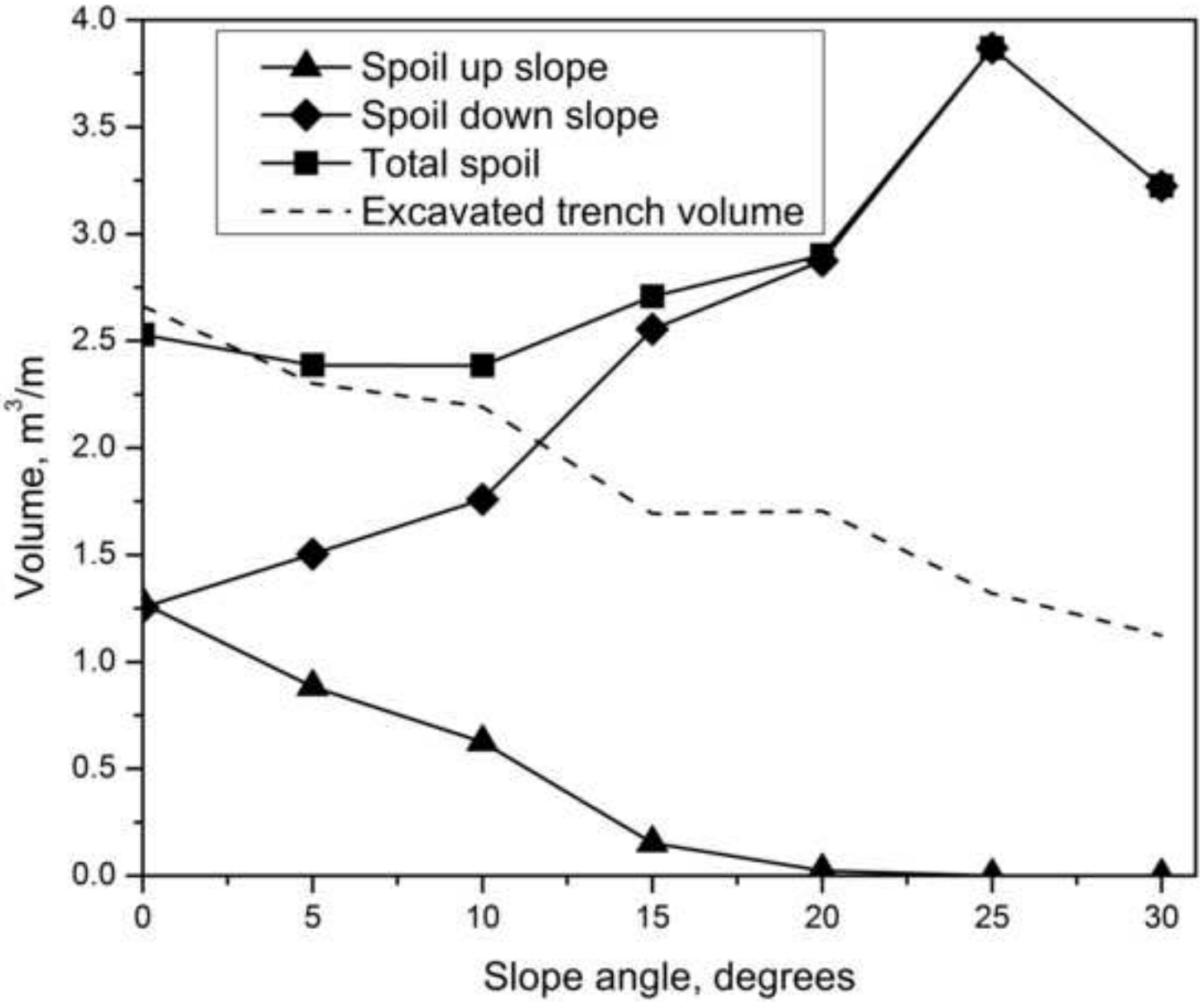

Fig. 16. Plan view of measured final trench position for all slo

Click here to download high resolution image

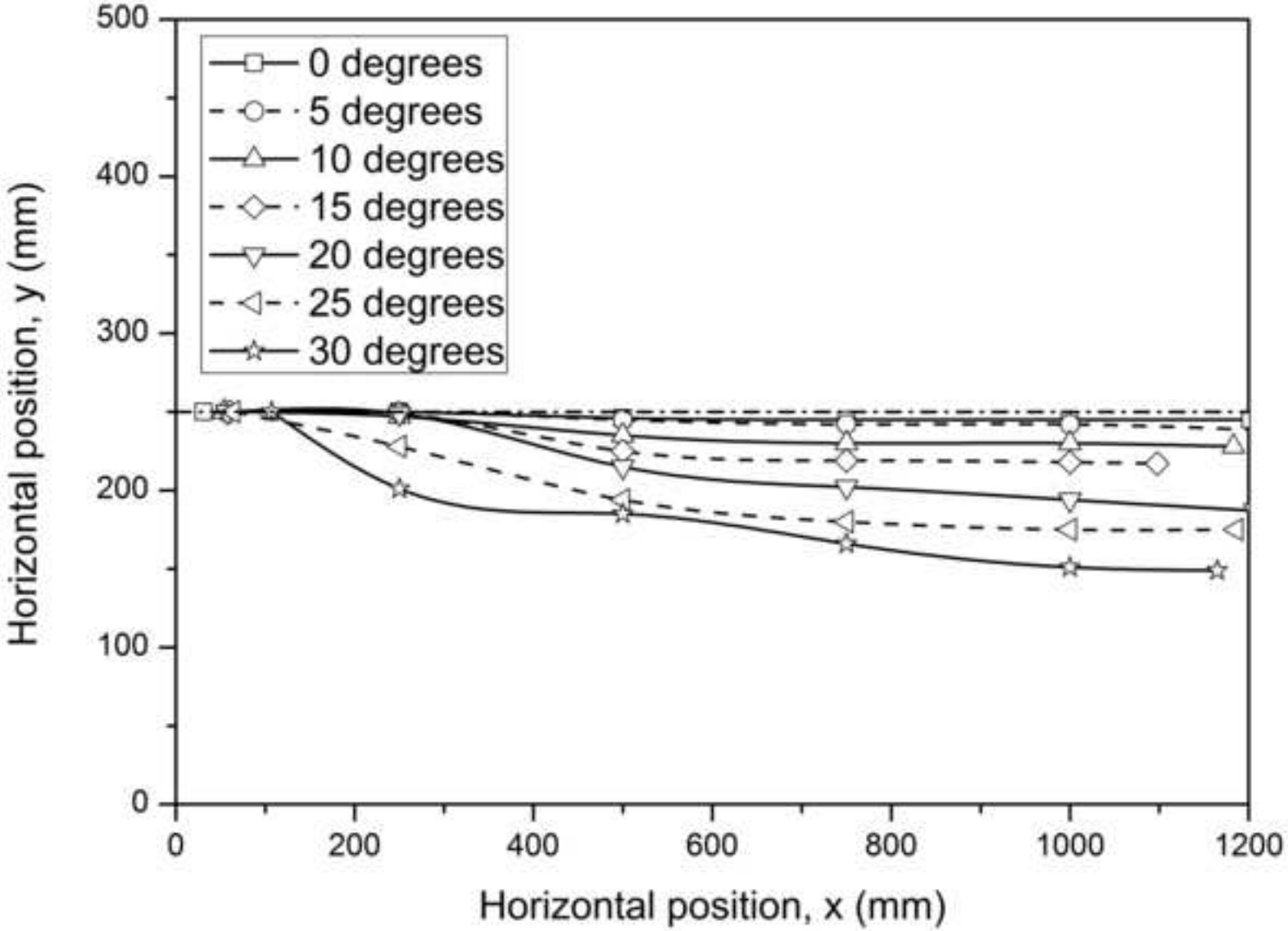

Fig. 8. Relationship between average tow force and trench depth

Click here to download high resolution image

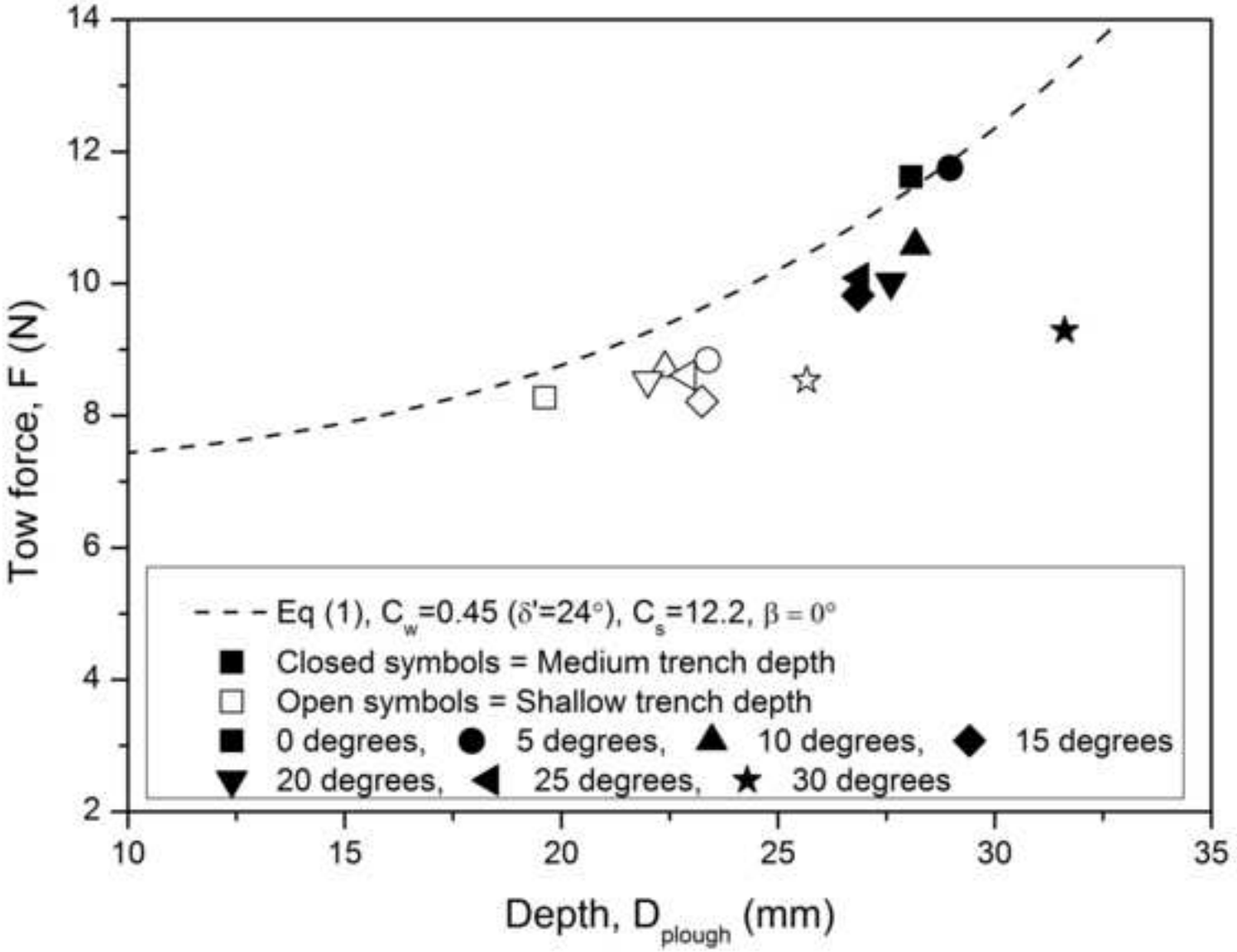

Fig. 15. Schematic plan view of trenching geometry. Note: all an
Click here to download high resolution image

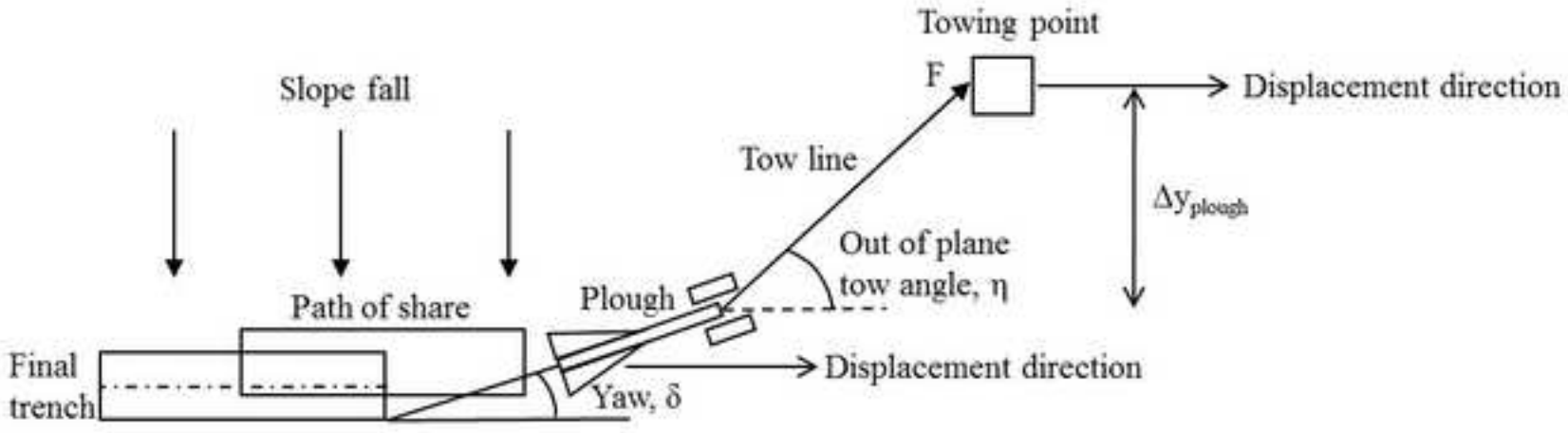

Fig. 17a. Pitch, yaw and tow angle variation with slope inclinat

Click here to download high resolution image

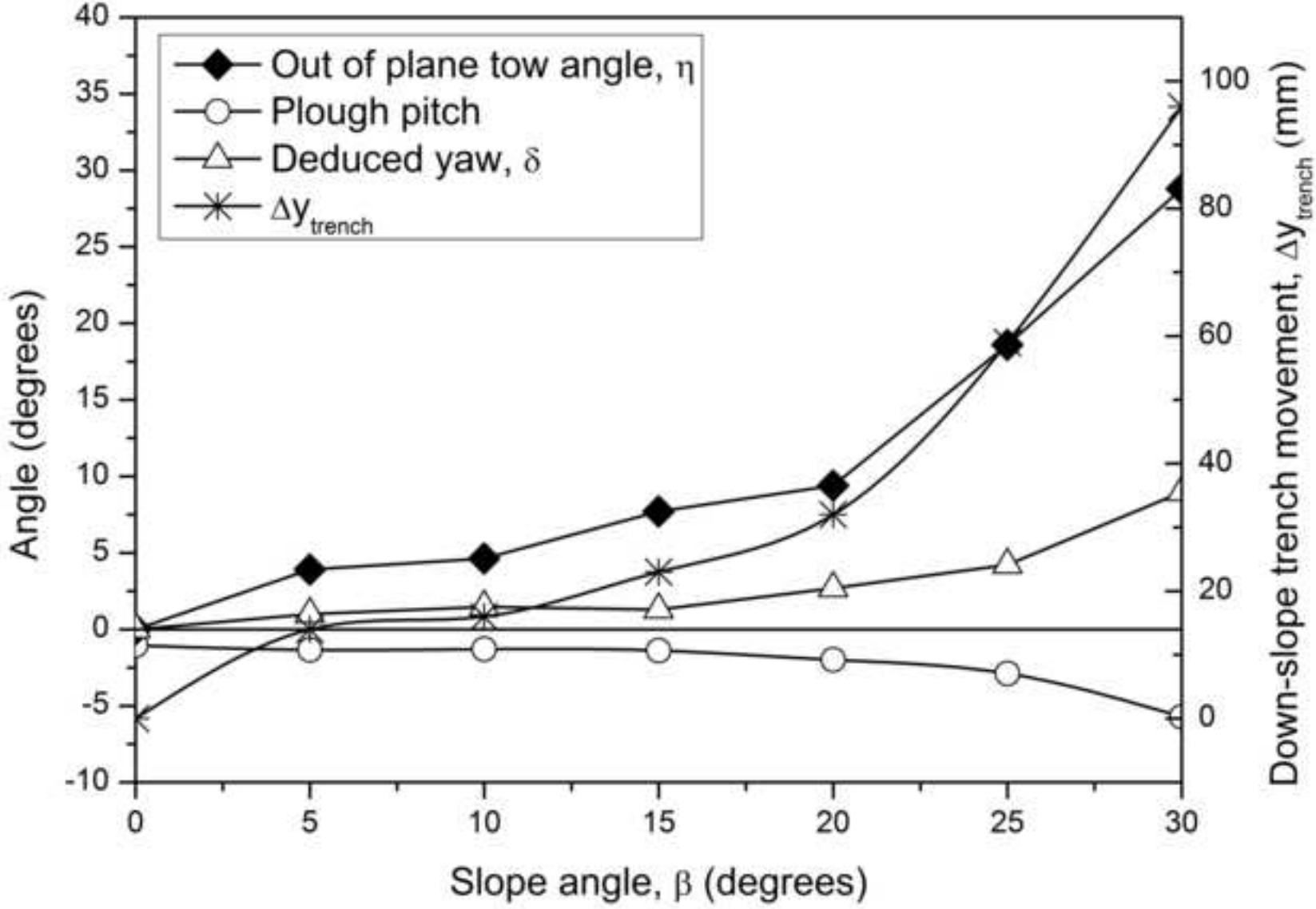

Fig. 17b. Pitch, yaw and tow angle variation with slope inclinat

Click here to download high resolution image

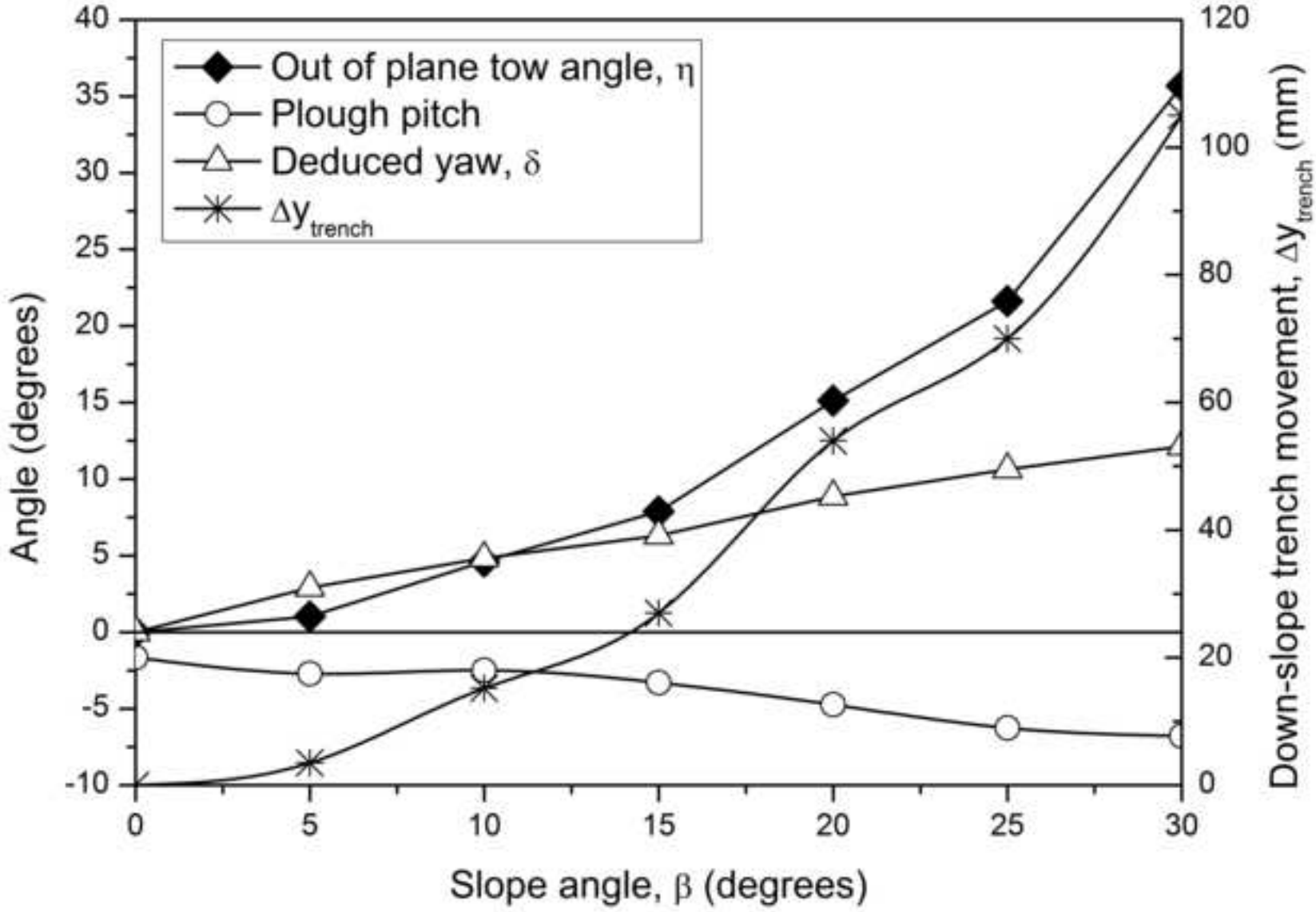

Table 1. Slope test conditions and average results obtained for

Table 1. Slope test conditions and average results obtained for shallow depth ploughing conditions.

Slope angle, β (°)	Plough depth (mm)	Trench depth (mm)	Tow force (N)
0	20.4	19.8	8.0
5	23.4	19.7	8.8
10	22.4	12.5	8.7
15	22.9	14.8	8.2
20	22.0	11.9	8.5
25	22.9	14.7	8.6
30	25.7	12.2	8.5

Table 2. Slope test conditions and average results obtained for

Table 2. Slope test conditions and average results obtained for medium depth ploughing conditions.

Slope angle, β (°)	Plough depth (mm)	Trench depth (mm)	Tow force (N)
0	28.1	28.0	11.6
5	29.9	24.8	11.8
10	28.2	17.6	10.6
15	26.9	11.3	9.8
20	27.6	13.1	10.0
25	26.9	10.2	10.1
30	31.6	10.3	9.3